Environment International 193 (2024) 109086

Contents lists available at ScienceDirect

Environment International

journal homepage: www.elsevier.com/locate/envint

Full length article

Aerosol particle number concentration, ultrafine particle number fraction, and new particle formation measurements near the international airports in Berlin, Germany – First results from the BEAR study

Simonas Kecorius [a,k,*], Susanne Sues [a,k], Leizel Madueño [b], Alfred Wiedensohler [b], Ulf Winkler [b], Andreas Held [c], Sabine Lüchtrath [c], David C. Beddows [d], Roy M. Harrison [d,e], Mario Lovric [f,g], Vanessa Soppa [h], Barbara Hoffmann [h], Miriam Wiese-Posselt [i], Andreas Kerschbaumer [j], Josef Cyrys [a]

[a] Institute of Epidemiology, Helmholtz Zentrum München - German Research Center for Environmental Health, Neuherberg, Germany
[b] Atmospheric Mircophysics, Leibniz-Institute for Tropospheric Research, Leipzig, Germany
[c] Environmental Chemistry and Air Research, Institute of Environmental Science and Technology, Technische Universität Berlin, Berlin, Germany
[d] National Centre for Atmospheric Science, School of Geography, Earth and Environmental Sciences, University of Birmingham, Edgbaston, United Kingdom
[e] Department of Environmental Sciences, Faculty of Meteorology, Environment and Arid Land Agriculture, King Abdulaziz University, Jeddah, Saudi Arabia
[f] Institute for Anthropological Research, Zagreb, Croatia
[g] The Lisbon Council, Brussels, Belgium
[h] Institute of Occupational, Social and Environmental Medicine, Centre for Health and Society, Medical Faculty and University Hospital, Düsseldorf, Heinrich Heine University Düsseldorf, Germany
[i] Institute of Hygiene and Environmental Medicine, Charité—Universitätsmedizin Berlin, Corporate Member of Freie Universität Berlin and Humboldt-Universität zu Berlin, Berlin, Germany
[j] Senatsverwaltung für Mobilität, Verkehr, Klimaschutz und Umwelt Referat Immissionsschutz, Berlin, Germany
[k] Environmental Science Center, University of Augsburg, Augsburg, Germany

ARTICLE INFO

Handling Editor: Xavier Querol

Keywords:
Exposure to particulate pollution
Particle number concentration
Particle number size distribution
Air traffic emissions
Airport emissions

ABSTRACT

Studies revealed airports as a prominent source of ultrafine particles (UFP), which can disperse downwind to residential areas, raising health concerns. To expand our understanding of how air traffic-related emissions influence total particle number concentration (PNC) in the airport's surrounding areas, we conduct long-term assessment of airborne particulate exposure before and after relocation of air traffic from "Otto Lilienthal" Airport (TXL) to Berlin Brandenburg Airport "Willy Brandt" (BER) in Berlin, Germany. Here, we provide insights into the spatial–temporal variability of PNC measured in 16 schools recruited for Berlin-Brandenburg Air Study (BEAR).

The results show that the average PNC in Berlin was 7900 ± 7000 cm^{-3}, consistent with other European cities. The highest median PNC was recorded in spring (6700 cm^{-3}) and the lowest in winter (5100 cm^{-3}). PNC showed a bi-modal increase during morning and evening hours at most measurement sites due to road-traffic emissions. A comparison between measurements at the schools and fixed monitoring sites revealed good agreement at distances up to 5 km. A noticeable decline in this agreement occurred as the distance between measurement sites increased. After TXL was closed, PNC in surrounding areas decreased by 30 %. The opposite trend was not seen after BER was re-opened after the COVID-lock-down, as the air traffic has not reached the full capacity yet. The analysis of particle number size distribution data showed that UFP number fraction exhibit seasonal variations, with higher values in spring and autumn. This can be explained by nucleation events, which notably affected PNC.

The presented findings will play a pivotal role in forthcoming source attribution and epidemiological investigations, offering a holistic understanding of airports' impact on airborne pollutant levels and their health implications. The study calls for further investigations of air-traffic-related physical–chemical pollutant properties in areas found further away (> 10 km) from airports.

* Corresponding author.
E-mail address: simonas.kecorius@helmholtz-munich.de (S. Kecorius).

https://doi.org/10.1016/j.envint.2024.109086
Received 2 May 2024; Received in revised form 27 September 2024; Accepted 17 October 2024
Available online 19 October 2024

1. Introduction

Aerosol particles, especially those produced in combustion processes, can have negative health effects (Kennedy, 2007). Studies in the field of toxicology and epidemiology suggest that exposure to black carbon (BC, airborne pollutant associated with combustion processes; acting as a carrier of carcinogenic chemicals) can lead to cardiopulmonary morbidity and mortality (Janssen et al., 2012). Health effects associated with airborne pollutants are significantly pronounced in urban environments, where the concentration of particulate matter (PM) often exceeds the guideline values set by the World Health Organization (2021). Here, airborne pollutants primarily originate from road transport (Rivas et al., 2020; Coelho et al., 2022), residential heating (Yun et al., 2020), and industry (Squizzato et al., 2017). In more recent studies, the scientific community has shown growing interest in the environmental and health impacts of air traffic and airport-related activities, which are associated with the release of elevated levels of airborne pollutants.

The smallest size fraction of ambient particulate air pollution, the ultrafine particles (UFP, particles with a diameter < 100 nm), have been hypothesized to be more toxic than larger particles, due to their large numbers and surface area, (HEI Review Panel on Ultrafine Particles, 2013). Due to their small size, the non-soluble UFPs are a serious health concern due to their ability to penetrate the bloodstream, causing negative effects on the respiratory and cardiovascular systems, as well as many other organs including the brain (Schraufnagel, 2020; Moreno-Ríos et al., 2022; and references there). The main sources of UFPs are combustion-related processes from industrial plants, power plants, and the transport sector, which is the dominant source of UFPs in urban areas. Multiple studies have shown that airport-related activities (e.g., plane engines, ground support equipment, such as baggage trolleys and fuel trucks) can lead to increased concentrations of total and ultrafine aerosol particles in the surrounding areas (Masiol et al., 2017; Tremper et al., 2022, Stacey et al., 2023) and are increasingly been recognized as potential sources of UFPs. This results in heightened exposure levels for airport employees (Møller et al. 2014). The airborne pollution originating from the airports consists of, among others, ultrafine aerosol particles, which are either directly emitted by the aircraft or produced in a nucleation process induced by jet engine oil vapors (Ungeheuer et al., 2022).

Short-term epidemiological studies have shown an association between aircraft-related (AC) UFP near a major airport and decreased lung function, as well as increased duration of ventricular repolarization in healthy adults (e.g., Lammers et al., 2020; Bendtsen et al., 2021; and references there). Janssen et al. (2019) examined the health effects of short-term exposure to UFP near Schiphol Airport in Amsterdam, Netherlands, in both children and adults. Their findings showed that on days with elevated exposure, children reported more respiratory issues and increased medication use compared to adults.

Some long-term studies showed an increase in malignant brain cancer risk (Wu et al., 2021) and increased rates of preterm birth (Wing et al., 2020). An extensive long-term study has been carried out on the health effects of ultrafine particles from air traffic by Janssen et al. (2022), The authors found suggestive evidence of adverse effects due to long-term exposure to UFP from aviation around Schiphol for several health outcomes (e.g., cardiovascular and respiratory disease, pregnancy, etc.). However, the knowledge about the aviation-related UFP effects on metabolic and neurodegenerative disease, as well as health effects on sensitive populations (e.g., children, elderly, and people with impaired cardiovascular and respiratory function), remain incomplete (Janssen et al., 2022). To increase the understanding of AC-UFP health outcomes, Janssen et al. (2022) called for studies on aviation-related UFPs, preferably around (international) airports with large populations of residents, and covering both high and low exposure scenarios in health studies.

From an exposure perspective, it is important to point out that airport-related health studies require data for source-specific physical–chemical properties of airborne pollutants. As described before, it is known that airport activities contribute strongly to UFP concentrations near the airfield. Nevertheless, it is important to consider that sources of UFP other than those associated with airports, such as road traffic (Trechera et al., 2023), urban new particle formation (Guo et al., 2020), and regional new particle formation (Cheung et al., 2013), may have a greater impact on personal exposure in environments situated at greater distances from the airport. In today's literature, there are few studies investigating airport emissions from the perspective of particle physical–chemical properties (e.g., Keuken et al., 2015; Masiol et al., 2016, 2017; Hudda et al., 2020; Tremper et al., 2022). In general, from source apportionment studies, it was found that airports contribute to 17——35 % PNC. It must be noted, however, that studies mentioned here have investigated airport source contributions at measurement sites found 1 to 2 km away from the airfield. So far, only few studies have reported the impact of airport emissions on particle size distribution (PSD) data at urban background measurement stations located few kms away from the airport (Cheung et al., 2011; Hudda et al., 2016; Keuken et al., 2015, Harrison et al., 2019, Riva et al., 2020). As concluded by Riva and colleagues (2020) further studies are needed to confirm the potential impact of aircraft emissions on air pollutant levels few kms away from the airport and isolate them from other sources.

The shutdown of Berlin Tegel "Otto Lilienthal" Airport (TXL) and the simultaneous opening of Berlin Brandenburg Airport "Willy Brandt" (BER) were planned for November 2020. This offered a unique opportunity to investigate the health effect of this measure on children living near the two airports and in control areas, which we assumed are not affected by the downwind from the two airports. Based on that, a prospective cohort study on children was developed and is still ongoing: "The Berlin-Brandenburg Air Study–a natural experiment investigating health effects from changes in airport-related exposures" (BEAR). BEAR is the first study in Germany to assess short- and long-term airport-related exposures – particularly of UFPs – and to investigate their associations with the pulmonary, cardiovascular, and cognitive health of primary school children. For more details on the BEAR study design, please refer to Soppa et al. (2023). Within the framework of this study measurements of outdoor PNC at the participating schools were conducted (short-term measurements). In parallel to the BEAR study, an exposure study "Ultra-fine dust pollution from airports in Berlin" (ULTRAFLEB, Diener at el., 2021) was conducted in Berlin. During this study, additional measurements of PSD were carried out at different locations in Berlin (long-term measurements). Long-term exposure to airport-related air pollutants is estimated by modelling within the ULTRAFELB project at children's homes and at schools.

The extensive measurements of PNC and UFP at multiple air quality monitoring sites, and schools in Berlin as part of the BEAR and ULTRAFLEB studies provide the unique opportunity to investigate the UFP and PNC levels at varying distances from the TXL and BER airports, i.e. spatial variation of PNC over the city of Berlin, the seasonal PNC patterns, and their relation to airports and local sources in Berlin. In this study, we present the first results of PNC measurements in multiple schools around two international airports and in control areas in Berlin, Germany, collected in the framework of the BEAR project in the period 2020–2022. The specific aims of the study are a) to investigate the spatial and temporal variation of particulate pollutants at various distances from the airports; b) to examine to what degree PNC measured repeatedly at multiple schools (short-term measurements) agree with measurements conducted at few fixed/semi-fixed (long-term measurements) air quality monitoring sites; and c) to investigate factors determining UFP number fraction in PNC measurements. The findings presented in this study provide a comprehensive overview of PNC values measured across Germany's capital, Berlin, and provide exposure data for BEAR and future follow-up epidemiological studies. Further analysis of the data, such as identification of airport-related physical–chemical properties of airborne pollutants, as well as source apportionment at

multiple measurement sites across Berlin, will be presented in a separate publication. The epidemiological analysis of the BEAR data is ongoing and will be published soon.

2. Methodology

2.1. Study design, measurement periods, instrumentation, and locations

Aerosol particle physical–chemical properties (e.g., total particle number and mass concentration, number size distribution, volatility, black carbon mass concentration) and gaseous pollutants (e.g. nitrogen oxides, ozone, carbon mono-, and dioxide) were measured at multiple locations in Berlin and Brandenburg, Germany, with varying distances to two international airports – TXL and BER. The TXL (52.56 N, 13.29E) is found approx. 9 km North-West of Berlin downtown. The TXL was closed on 8 November 2020 and decommissioned as an airfield on 4 May 2021. All traffic from TXL was transferred gradually to BER, which was opened for commercial traffic on 31 October 2020. BER (52.37 N, 13.51E) is found approx. 18 km southeast of Berlin downtown. In the year 2022, the airport recorded over 19.8 million passengers. Further details about airports, e.g., operated runways, takeoff, and landing-routes, etc., can be found in BER annual reports (https://corporate.berlin-airport.de/en/company-media/media-portal/publikationen.html, and https://corporate.berlin-airport.de/de/umwelt/luft.html, accessed 28 March 2023).

The primary emphasis of this study is on three-year (2020–2022) measurements of PNC and UFP at multiple air quality monitoring sites, and schools in Berlin found at varying distances from the TXL and BER airports and in control areas. The measurement domain is shown in Fig. 1. The PNC measurements took place in 16 separate locations (schools) with distances to TXL and BER airports spanning from 3 to 14 km. The detailed description of some measurement sites can be found in supplementary information (SI).

The aerosol data analyzed in this study include PNC and particle number size distribution (PNSD) obtained from four different data sources: 1) measurements of PNC at multiple schools; 2) measurements of physical–chemical properties of air pollutants from mobile measurement container and trailer; 3) long-term air quality measurement sites operated by airport authorities; and 4) long-term air quality measurements at two state-operated air quality monitoring station. A description of aerosol instrumentation and each data provider is available in SI.

2.2. Changes in study design due to COVID-19

The BEAR and ULTRAFLEB studies were originally designed to capture abrupt changes in airport-induced physical–chemical aerosol particle properties related to the planned TXL closure and BER opening. The TXL airport closure took place on 8 November 2020 (decommissioned as an airfield on 4 May 2021), while the BER airport was opened on 10 October 2020 (for commercial traffic on 31 October 2020). It must be noted that before the official inauguration of BER airport, the airfield served as Berlin-Schönefeld airport, a smaller local airport, signifying a continuous presence of air traffic even before BER's opening (see Fig. S1). The rise of an infectious disease caused by the severe acute respiratory syndrome coronavirus 2 (SARS-CoV-2, also known as COVID-19) has caused changes in air traffic intensity for a period from approx. 1 March to 1 July 2020. The TXL airport closure, BER opening, and COVID-19 pandemic created a complicated condition during which air traffic flow suddenly decreased/increased, having an observable influence on airport-related PNC emissions. Due to restrictions in response to the COVID-19 pandemic, some of the planned measurements were halted during the intermittent lockdown periods. This particularly affected the PNC measurements at schools. As a result, the majority of analyzed data in this paper is from the post-COVID-19 period, when air traffic has not yet fully recovered to pre-pandemic levels. In light of the constrained dataset, we were able to capture several instances in which a comparative analysis of physical particle properties was conducted across the following scenarios: a) examination of PNC values at T1 before, during, and after the TXL closure and the COVID-19 pandemic; b) assessment of PNC in the proximity of TXL airport before and after the airport's closure; and c) evaluation of PNC in the vicinity of BER airport before and after the airport's inauguration (Fig. 2).

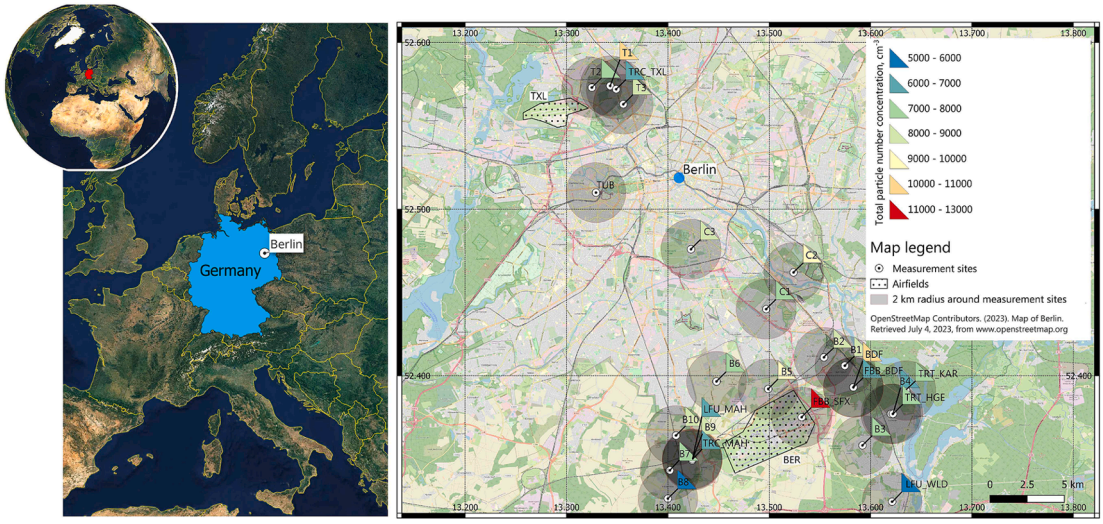

Fig. 1. Short- and long-term measurement site locations in Berlin and Brandenburg, Germany. The letter "T" indicates sites near the TXL airport, with the accompanying number serving as an identifier for ordering purposes, while the letter "B" designates sites near the BER airport. Each six-letter code has the following meaning: TRC_TXL – TROPOS measurement container near the TXL; TRC_MAH – TROPOS measurement container in Blankenfelde-Mahlow; TRT_KAR – TROPOS measurement trailer in Karolinenhof; TRT_HGE – TROPOS measurement trailer in Eichwalde, Brandenburg; FBB_BDF – measurement site in the district of Bohnsdorf, operated by the Berlin Brandenburg Airport (FBB); FBB_SFX – FBB measurement site within the BER airport; LFU_MAH – measurement site in Blankenfelde-Mahlow, operated by the Brandenburg State Office of Environment (LfU); and LFU_WLD – LfU measurement site in Wildau. The TXL and BER airport areas are shown with a dotted pattern. The grey circular (four kilometers in diameter) shaded area around each measurement site is used to calculate the land use index based on the Coordination of Information on the Environment Land Cover 2018 database, available at https://land.copernicus.eu (accessed 20th October 2023). The color-coded triangles show mean PNC, averaged over the whole measurement period.

Due to data availability constraints, we dedicated a section for the comparative analysis of the physical properties of airborne pollutants within the three scenarios outlined earlier. The rest of the analysis will not distinguish between periods before and after airport closure/opening, and before, during, and after the COVID-19 pandemic. This is primarily because during the COVID-19 pandemic, the air traffic, although decreased, did not halt completely (cargo planes were still in operation).

2.3. Data evaluation and analysis

The PNC and ground-level meteorological parameters were carried out using three identical condensation particle counters (CPC, 50 % cut-size 7 nm, model EDM 465; Grimm, Germany). All PNC measurements from schools were manually screened for outliers and bad scans. This included singular concentration spikes (sometimes order of magnitude higher than the running average; see Fig. S2), zero and/or missing values due to instrument malfunction (e.g., power-offs, working liquid delivery failure, etc.), as well as the instances when the instrument meteorological sensors were not connected/properly aligned to the north. All such measurement periods were tagged with an identifier, which was later used for data filtering. The aerosol measurement data received from the Leibniz Institute for Tropospheric Research (TROPOS), Flughafen Berlin Brandenburg GmbH (FBB), and the Brandenburg State Office of Environment (Landesamt- für Umwelt Brandenburg, LFU) were used as provided with no additional data quality assessment. Shortly, the measurements using TROPOS container and trailer, relevant to this study, included PNC and PNSD. The PNC was measured using CPC (cut-size 7 nm, model 3010; TSI, USA). The PNSD was measured in an electric mobility size range from 10 – 800 nm (using TROPOS-built mobility particle size spectrometer, MPSS). The PNSD measurements (in an electric mobility size range 10 – 1000 nm) at FBB BDF station were performed using scanning mobility particle spectrometer (SMPS, GRIMM, Germany). The PNC at FBB operated sites were calculated from measured PNSDs (Particle Number Size Distribution). For a more detailed description of the instrumentation used (including their comparability) please refer to SI.

2.4. Statistical analysis

After data evaluation, spatial and temporal variation of aerosol particle physical properties and statistical analysis were performed using the open-source programming language and software environment R (R Core Team, 2013; version 4.2.2). Open-source tools for air quality data analysis (Carslaw and Ropkins, 2012) and custom functions were used to investigate PNC and PNSD data. For spatial data representation, a quantum geographic information system (QGIS Development Team, 2022) was used. Other figures were made using R and a cross-platform scientific application for data analysis and visualization (QtiPlot, 2008; version 0.9.8.3).

To evaluate both measurement quality as well as to examine to what degree long-term measurement sites can be represented by short-term-multiple-location measurements, we used the metrics of precision, bias, the coefficient of determination (R^2), and concordance correlation coefficient (CCC). In this section, we shortly present the formulation for the metrics used. We begin with the precision, which can be described as a measure of mutual agreement among individual measurements of the same property (Camalier et al., 2007; Solomon et al., 2020) and can be calculated using Eq. (1):

$$precision = \frac{\sqrt{\left(n\cdot\sum_{i=1}^{n} RPD_i^2\right) - \left(\sum_{i=1}^{n} RPD_i\right)^2}}{(2n(n-1))}\cdot\sqrt{\frac{(n-1)}{\chi^2_{(0.1,n-1)}}} \quad (1)$$

where n is the number of data pairs from two condensation particle counters (CPC), $\chi^2_{(0.1,n-1)}$ is the 10th percentile of a chi-squared distribution with n-1 degrees of freedom, and RPD is the relative percentage difference. The RPD metric measures the deviation of the evaluated CPC from the reference CPC as a percentage of the reference value and can be calculated using Eq. (2):

$$RPD = \frac{(X_i - Y_i)}{(Y_i)}\cdot 100 \quad (2)$$

where X_i is the PNC of the CPC to be evaluated, and Y_i is the PNC from the reference CPC. Precision shows how consistent and repeatable two measurements are, regardless of whether they are close to the true value. In the case of our work, higher precision values show higher disagreement. The measure describing how well measurements represent a true value is called bias. The bias can also be described as the positive and negative deviation from the true value (expressed in percentage). We calculated the bias using Eq. (3):

$$bias = \frac{1}{n}\sum_{i=1}^{n} RPD \quad (3)$$

The upper and lower bias confidence intervals (UCI and LCI, respectively) were calculated as follows:

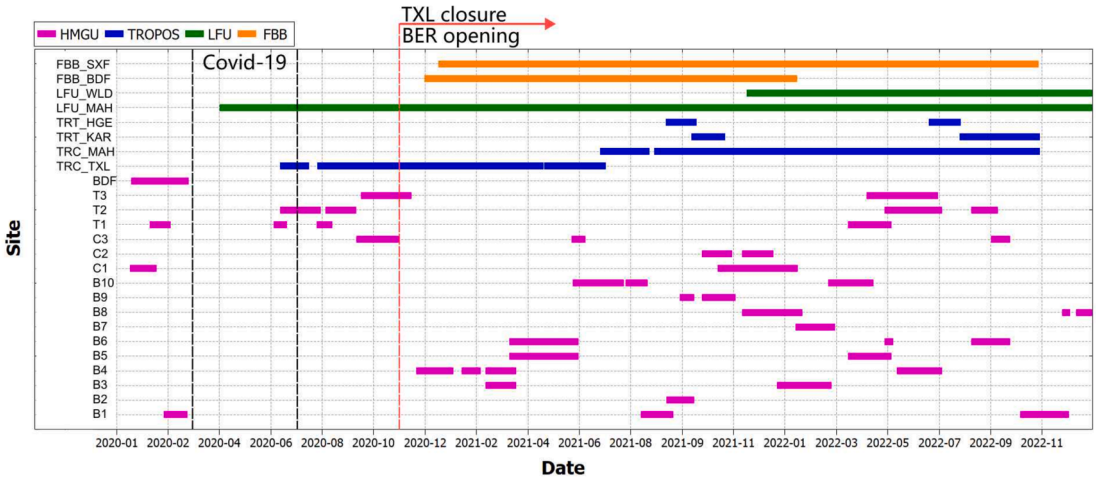

Fig. 2. Data availability graph indicating measurement period and location. The vertical dashed lines indicate periods when the flight activity was reduced (Fig. S1) in both TXL and BER airports (due to COVID-19; black lines), as well as the closure of TXL/opening of BER airports (red line). Here, the HMGU stands for measurement sites operated by Helmholtz Munich; TROPOS – Leibniz-Institute for Tropospheric Research; LFU – Brandenburg State Office of Environment; and FBB – Airport Berlin Brandenburg. (For interpretation of the references to color in this figure legend, the reader is referred to the web version of this article.)

$$UCI = bias + t_{0.95,df} \cdot \frac{s_d}{\sqrt{n_i}} \quad (4)$$

and

$$LCI = bias - t_{0.95,df} \cdot \frac{s_d}{\sqrt{n_i}} \quad (5)$$

where $t_{0.95,df}$ is the 95th quantile of a t-distribution with n-1 degrees of freedom, and s_d is the standard deviation of *RPD*. The absolute (or signed) bias was calculated using Eq. (6) and (7):

$$|bias| = \frac{1}{n} \cdot \sum_{i=1}^{n} |RPD_i| + t_{0.95,n-1} \cdot \frac{AS}{\sqrt{(n)}} \quad (6)$$

$$AS = \sqrt{\frac{n \cdot \sum_{i=1}^{n} |RPD_i|^2 - \left(\sum_{i=1}^{n} |RPD_i|\right)^2}{n(n-1)}} \quad (7)$$

The sign direction (positive or negative) of absolute bias is chosen based on the 25th and 75th percentiles of the *RPD*. The $|bias|$ upper bound should be flagged as "+" if both percentiles are "+" and "-" if both percentiles are "-". The $|bias|$ would not be flagged if the 25th and 75th percentiles had different signs.

The R^2 measures the goodness-of-fit of the regression model (between PNC measured at two sites). Although R^2 can indirectly provide information about the precision of a regression model, it does not provide information about whether the predicted values are close to the true values or the actual accuracy of individual predictions. The CCC, on the other hand, is a statistical measure that can be used to quantify the degree of agreement between two data sets, considering both precision and accuracy. The CCC (Lin, 1989), was calculated using the R package Icc (Oliveira et al., 2020) and can mathematically be expressed as:

$$CCC = \frac{2 \cdot \rho \cdot \sigma_{PNC1} \cdot \sigma_{PNC2}}{\sigma_{PNC1}^2 + \sigma_{PNC2}^2 + (\mu_{PNC1} - \mu_{PNC2})^2} \quad (8)$$

where μ, σ and ρ are mean, variance, and Pearson correlation coefficient of PNC measurements from two CPCs (PNC_1 and PNC_2), respectively.

The moving window percentile, as presented in Section 2.4 (Figs. 6 and 7), was calculated using the caTools package within the open-source programming language and software environment R (available at https://cran.r-project.org/web/packages/caTools/, last accessed on September 3, 2024).

We use multiple metrics to assess comparability between measurement sites to minimize the risk of incorrect conclusions. If one metric indicates comparability while another raises concerns, it triggers further investigation. This, however, resulted in many descriptive parameters (see Table S1), which will be not provided in the main text and can be found in the SI.

Before discussing the results, it is worth defining the limits at which the data between the two sites can be seen to be in good agreement. Starting with R^2, Tremper et al. (2022) adopted R^2 values from the British Medical Journal (BMJ 2021), calling the correlation strong and very strong when the R^2 values are in the ranges of 0.60–0.79 and 0.8–1.0, respectively. In other research disciplines, e.g., economics or social sciences, the R^2 values for acceptable correlation are from 0.5 to 0.75 (Henseler et al., 2009; Ozili, 2023). In this work, we use the limit value of $R^2 > 0.75$ to indicate measurement sites that are in good agreement. The ranges for CCC were proposed by McBride (2005), who suggested naming comparison between two data sets as poor if the CCC < 0.9. However, within the context of atmospheric science, this stringent criterion may potentially impede our ability to discern the extent to which short-term measurement sites can be effectively characterized by long-term monitoring stations. Other interpretations of CCC values do exist in scientific literature. For example, Kim and Lee (2022) refer to data sets to be in good agreement if CCC is above 0.75. Barlund et al. (2008) showed agreement between two data sets as substantial with a CCC value of approx. 0.65. In this work, we set a limit of CCC > 0.6 to evaluate if the two data sets are in good agreement. We selected this threshold due to the greater variability observed in atmospheric science data and use it primarily for exploratory analysis rather than for decision-making purposes. The acceptable PNC precision values for comparing two measurement sites are unfortunately not available in the literature. We chose it to be 30 % based on the combined uncertainty between CPC precision (13 %) and recommended $PM_{2.5}$ precision values reported by Camalier et al. (2007) and Considine et al. (2021, and references there) for regulatory monitoring. It must be noted, however, that firstly – precision in regulatory monitoring refers to measurement site instrument comparison to the standard, while in our study, we compare two measurement sites located several kilometers apart; and secondly – the PNC, largely comprising of UFP, is much more variable compared to PM mass concentration, which is unaffected by UFP variation. In other words, our chosen precision value of 30 % can be considered a more stringent limit for two measurement site comparability. The same is valid for the bias – we chose the limit value of ± 30 % to indicate good agreement between two measurement sites.

3. Results and discussion

3.1. Overview of measurements

The overview of total PNC spanning over two years and 25 measurement locations, with varying distances to the international airports, is given in Fig. 2 and Table 1. The overall average PNC of Berlin and Brandenburg (calculated from all measurement sites and measurement periods) was 7900 cm^{-3} (with a standard deviation of 7000 cm^{-3}). Corresponding PNC median and 25th/75th percentile values were approx. 6200 cm^{-3} and 4100/9500 cm^{-3}, respectively. The median PNC values align closely with those reported in urban settings, as seen in other urban areas such as Athens and Prague (Rose et al., 2021). Our findings position the PNC concentration at an intermediate level among previously documented urban areas, with a ranking of Leipzig (urban background, Germany) < Berlin (this study) < Ispra (Italy) < Granada (Spain) < Dresden (Germany).

When looking at the overall average PNC per measurement site, it can be seen that the three highest average concentrations (±standard deviation) were recorded at FBB SXF (13120 ± 13190 cm^{-3}), BDF (10350 ± 8290 cm^{-3}), and T1 (10020 ± 8230 cm^{-3}) – sites located in close proximity to an airfield. The highest mean and median PNCs and standard deviation values were found at FBB SXF, a measurement site directly located inside the airport. The other two sites, BDF and T1, despite showing high PNC concentrations, were located further away from the respective airfields (5.7 and 4.0 km, respectively). The lowest average (± standard deviation) and median PNC were recorded at site B8 and were 8740 ± 4890 cm^{-3} and 4490 cm^{-3}, respectively. The B8 measurement site is 8.8 km southwest of BER airport. From Table 1 it can be seen that there are other measurement sites located further away from an airfield (compared to B8), however, exhibiting higher PNC concentrations (e.g. C2, C3). This may be due to the fact that the latter measurement sites were established towards the city center of Berlin, which is more affected by road traffic-related emissions, compared to sites situated in a more background environment (e.g., B8). It is also worth noting that the PNC measurements at schools were not continuous. Therefore, averages presented in Table 1 may cover only one season and thus be biased. We therefore further discuss the results by segregating PNC into different seasons. The highest median seasonal concentration in Berlin and Brandenburg was measured in spring and was approx. 6700 cm^{-3}, followed by autumn – 6500 cm^{-3}, and summer – 6300 cm^{-3}. The lowest seasonal PNC in Berlin and Brandenburg was measured in winter at 5100 cm^{-3}. Compared to long-term urban PNC measurements reported by Rose et al. (2021), our results (spring showing the highest median PNC; winter – the lowest) are unique, as none of the previously reported PNC values from European cities had

Table 1
The PNC statistics (based upon hourly averaged data; mean ± standard deviation, median, 25th/75th percentile, and number of data points) for all measurement sites are indicated in Fig. 1. The distance to an airfield (both BER and TXL) in kilometers is also given in the table. The measurement sites located at schools is indicated by "*".

Site	Mean ± sd	Median	25th / 75th percentile	Distance to airfield	n
B1*	8180 ± 6900	6110	4020 / 9670	6.2 km to BER	2261
B2*	8230 ± 5200	6900	4740 / 9820	5.8 km to BER	547
B3*	7790 ± 5600	6340	4140 / 9800	5.4 km to BER	1925
B4*	6820 ± 4480	5700	4020 / 8360	7.4 km to BER	2792
B5*	9330 ± 6210	7660	5180 / 11770	3.1 km to BER	2551
B6*	7580 ± 4320	6550	4630 / 9270	5.6 km to BER	2535
B7*	7460 ± 5230	6120	3740 / 9600	8.0 km to BER	872
B8*	5200 ± 3310	4490	2850 / 6780	8.8 km to BER	1585
B9*	8280 ± 5260	6980	4700 / 10,430	6.3 km to BER	913
B10*	8320 ± 5210	7140	4860 / 10,220	7.2 km to BER	2635
C1*	7660 ± 4890	6510	4440 / 9250	8.4 km to BER	2502
C2*	9640 ± 5890	8190	5740 / 11,770	10.8 km to BER	1259
C3*	8740 ± 4890	7760	5650 / 10,650	13.8 km to BER	1477
T1*	10020 ± 8230	7490	5070 / 11,960	4.0 km to TXL	1730
T2*	7930 ± 5000	6630	4600 / 9680	2.9 km to TXL	3367
T3*	8280 ± 5570	6920	4950 / 9990	4.6 km to TXL	2779
BDF	10350 ± 8290	7710	5340 / 12,140	5.7 km to BER	1268
TRC TXL	6500 ± 3780	5600	3890 / 8040	4.0 km to TXL	7318
TRC MAH	6180 ± 4480	5090	3280 / 7670	6.3 km to BER	10,826
TRT KAR	7410 ± 4430	6220	4590 / 8820	8.9 km to BER	2613
TRT HGE*	7440 ± 4060	6350	4810 / 8810	7.4 km to BER	1478
LFU MAH	6790 ± 4580	5670	3820 / 8350	6.3 km to BER	23,243
LFU WLD	5870 ± 3330	5120	3640 / 7200	8.8 km to BER	9177
FBB BDF	6440 ± 3840	5730	3970 / 8180	5.7 km to BER	15,978
FBB SXF	13120 ± 13190	9230	5890 / 15,510	0.0 km to BER	16,025

similar seasonal patterns. It must be noted, however, that our reported values stand for the median over multiple sites (representing both urban and urban background environments). Looking at PNC values from separate sites, the highest average PNC was recorded in spring at C3 with approx. 23000 cm^{-3} (with a standard deviation of 13000 cm^{-3}; median and 25/75th percentiles of 19300 cm^{-3} and 14700/22200 cm^{-3}, respectively). Interestingly, this site is found furthest (14 km) away from the BER airport and closest to the Berlin city center. High PNC recorded here may be a result of road-traffic emission and related new particle fromation through increased growth rates (Brean et al., 2024). The second highest seasonal PNC was recorded in autumn at FBB SXF and was approx. 16500 cm^{-3} (with a standard deviation of 15700 cm^{-3}; median and 25/75th percentiles of 11000 cm^{-3} and 6700/19700 cm^{-3}, respectively). From here, it can already be seen that in an urban environment, depending on the season, PNC not related to air traffic can be noticeably higher than that observed inside the airport. The lowest mean values of PNCs were recorded at TRC MAH and LFU WLD in winter, and B1 in summer, and were on average below 5000 cm^{-3}.

An informative way to look at PNC seasonal variability is to calculate the ratio of the maximum and minimum seasonal medians (SeasC; Rose et al., 2021). Seasonal PNC variation can be categorized as low when SeasC values are below 2, while values > 2 denote high seasonal variability. The ratio of the smallest and the largest seasonal medians can be found in SI Fig. S3. Out of 22 sites, 17 showed only limited seasonal variability, with SeasC values being < 1.5. It is hard to say what the reason is for a stable PNC during different seasons. One cause may be related to measurement site locations. Rose et al. (2021) explained low seasonal variability in urban sites by stable traffic-related emissions. However, we did not see such a clear pattern in our case of multiple measurement sites in Berlin. As an illustration, we consider two measurement sites, FBB SXF and TRT KAR, both exhibiting SeasC values of 1.2–1.3. The former, FBB SXF, is situated near BER airport and major highways, while the latter, TRT KAR, is enveloped by green areas and residential buildings. In such a case, based on earlier hypothesis, we would expect that FBB SXF and TRT KAR would show noticeably different seasonal variation in PNC. Among the five sites, B4, B7, T2, TRC MAH, B1, and C3, SeasC values ranged from 1.9 to 2.6. Notably, three of these sites recorded their highest PNC levels during the spring months. It is specifically pronounced for a C3 measurement site, found in a densely populated neighborhood, with traffic-intensive roads (e.g., A100 motorway) nearby. The PNC increase seen during the spring supports the role of secondary aerosol processes (new particle formation, NPF), which can be an important source of particles in the urban atmosphere (Salma et al., 2014; Brines et al., 2015). It is essential to highlight that a comprehensive analysis of the underlying reasons for varying seasonal PNC trends across all Berlin measurement sites was not possible. This limitation arises from the fact that PNC measurements at different sites were conducted for specific periods, and these periods did not uniformly span over all seasons.

3.2. *The relation between PNC and distance of measurement sites from an airfield*

As aviation is a strong source of PNC (e.g., Hudda et al., 2018; Ungeheuer et al., 2022; Riley et al., 2021 and references therein), a scientific question is how PNC values change with increasing distance to an airfield. A comprehensive review presenting the impact of commercial airplane activity on air quality near airports by Riley et al. (2021) suggests that the elevated PNC can be detected up to 18 km downwind from the airport area. It is reasonable to assume that there shall be a gradual decrease in PNC with increasing distance to the airfield. To investigate how PNC depends on the measurement site distance to the airport area in Berlin and Brandenburg, we have calculated the straight-line distance from the closest airfield to all measurement sites and plotted it against PNC (Fig. 3, Fig. S4 – S5).

In case of autumn mean PNC (represented by the black circles in Fig. 3, as well as the black dashed line), there is an observable decrease of PNC from the mean value of 16500 cm^{-3} (with a standard deviation of 15700, median and 25th/75th percentiles of 11,000 and 6700/19700 cm^{-3}; measured at FBB SXF) to the mean value of 8000 cm^{-3} after 5 km from an airfield. During other seasons, however, such a decrease is much less pronounced. Furthermore, there are cases when PNC measured further away from an airport showed higher PNC compared to those measured at the airfield. For example, in winter, PNC measured at T1 is 30 % higher than that measured at the airport (FBB SXF). Please note, however, that in Fig. 3, the T1 distance to an airport stands for the measurement site distance to TXL airport (not BER, where the FBB SXF is found). Another example is measurement sites B1 (6.2 km to an airport) and C3 (13.8 km to an airport), which showed respectively similar and 96 % higher PNC than that measured inside the airport. Suggesting that in winter and spring, there are instances when measurement sites found

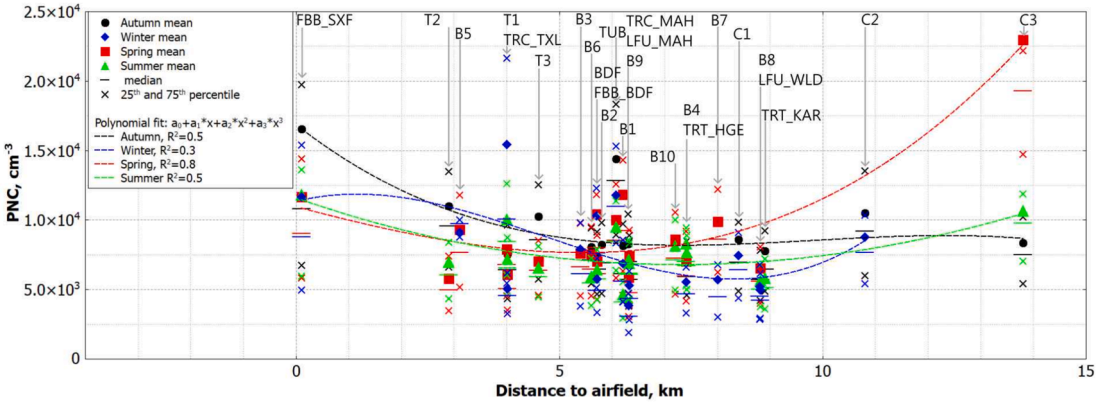

Fig. 3. The average (as colored ○, ◇, □, △), median (as "–"), and 25th/75th percentiles (as "x") PNC as a function of distance to the airfield segregated by season. Please note that for the measurement sites T1, T2, TRC TXL, and T3, the distance to the airfield represents distance to TXL airport, while for the remaining measurement sites – a distance to BER airport. A season-segregated polynomial fit is shown as dashed lines (assorted colors represent a different season). A polynomial fit was chosen to illustrate both PNC decrease and increase with changing distance from an airfield. The fit parameters are available in SI Table S2.

further away from an airfield experience similar or even higher PNCs without being directly exposed to air-traffic emissions. Other known pollutant sources that may affect PNCs include (for winter seasons) residential heating (Yu et al., 2019), and new particle formation (for spring and summer months, Sulo et al., 2021). When considering overall mean concentration per measurement site (without segregating between different seasons; Fig. S4), the PNC decrease with increasing distance from an airport becomes more visible and exhibits moderate strength linear relation with $R^2 = 0.5$ and a PNC decrease of approx. 520 cm^{-3} km^{-1} (after removing C2 and C3 results from the analysis due to evidently different values and PNC daily patterns). This relation becomes less clear after the 10 km mark when PNC suddenly increases from approx. 6000 cm^{-3} (at 9 km from an airport) to above 8000 cm^{-3} (beyond 10 km from an airport).

As mentioned previously, it is worth noting that the mean (as well as median and percentile) PNC values used here for a discussion do not represent full-year measurements. For this reason, PNC values from some measurement sites (e.g., covering summer and winter months) may be biased with respect to other sites (e.g., covering only spring months). In other words, only an episodic measurement, not covering full-year continuous PNC monitoring may falsely represent occurring PNC trends. The PNC scaling correction can be applied to all measurement sites based on long-term monitoring data (usually taken from state-operated environmental monitoring stations). Such correction was successfully applied to particle mass concentration measurements in some earlier studies (e.g., Wolf et al., 2017). However, the application and reasoning of such corrections is beyond the scope of this work. A more accurate picture of PNC dependence on the distance to an airfield can be drawn from a few long-term measurements available for this study. When analyzing PNC values from measurement sites that cover all seasons (TRC TXL, FBB BDF, TRC MAH, LFU MAH, and LFU WLD), we can see that in fact there is a slight decrease in PNC with increasing distance to an airfield (145 cm^{-3} km^{-1}, Fig. S5). The more distant sites (e.g., LFU WLD, LFU MAH, and TRC MAH) are located away from the Berlin city center, in an urban background, which may influence our results (having lower PNC values compared to Berlin urban environment).

3.3. Hourly PNC variations

The season-segregated all measurement site average hourly variation of PNC is shown in Fig. 4. During all seasons, there are two distinct PNC increases during morning (approx. 5:00 to 8:00) and evening (approx. 19:00 and 22:00) hours. Such PNC bi-modality was previously seen in many urban environments and can be associated with rush hours and road-traffic-related emissions (e.g., Hussein et al., 2004; Wiesner et al., 2020; Casquero-Vera et al., 2022). A slight decrease in PNC during midday hours can be related to the development of mixing layer height, during which PNC is distributed through a greater volume, thus reducing its concentration. Contrarily, the higher PNC at night may be related to the formation of a shallower and more stable nocturnal boundary layer (Casquero-Vera et al., 2022; Seidler et al., 2023). When it comes to air traffic, Trebs et al. (2023) showed that the daily pattern of flight activity strongly resembles that of road traffic (e.g., Wiesner et al., 2020). This can be confirmed with our flight data from TXL and BER airports (see Fig. 5 and Fig. S1). The airport activity sharply increases from 6 AM, reaches its maximum by 8 AM, where it stays for the most part of the day, and decreases to a minimum by 10 PM. It means that air- and road-traffic-related emission patterns are intertwined, making it a complex task to resolve the contribution of diverse sources to PNC. This is especially true when PNCs are measured further away from an airfield.

Furthermore, as the airports are mostly found outside the cities, airplane emissions are diluted by near-surface turbulence, effectively reducing PNC downwind. Trebs et al. (2023) showed that because of airplane plume dispersion, the UFP concentrations measured in the vicinity of an airport were reduced during the day, even when the airport activity was at its maximum. To investigate the link between PNC and flight activity at TXL and BER airports, we have calculated a site-specific Pearson correlation coefficient for all hours of the day (Fig. 5). Initially, the outcomes from TXL and BER airports seem to show clear disparities. For the case of BER airport, the PNC from six measurement sites (BDF, B1, LFU MAH, B4, C1, and C3) showed only a weak correlation (r of approx. ± 0.4; only during morning hours) with airport activity. Interestingly, negative weak or no correlation was seen from 10 AM throughout the rest of the day, despite airport activity being at its highest. Firstly, increased mixing layer height during the midday hours and strong local road traffic emissions may surpass the diluted PNC originating from the airport. Secondly, due to insufficient measurement duration, there may not have been enough favorable downwind conditions to help transport airport emissions to the measurement sites.

In most previously published studies, PNC increases due to airport activities were investigated with respect to the wind sector that includes an airport (e.g., Hudda et al., 2018; Seidler et al., 2023). It is a reasonable approach to show the contribution of airport-related activities to PNC in the surrounding areas. However, the frequency of instances when the prevailing wind is coming from an airport must also be shown. This is important because when studying airport pollution from distant sites, measurements may coincide with prevailing wind directions that do not include airport emissions. For example, in a study by Seidler et al. (2023), authors found that in an airport surrounding area, only up to 14

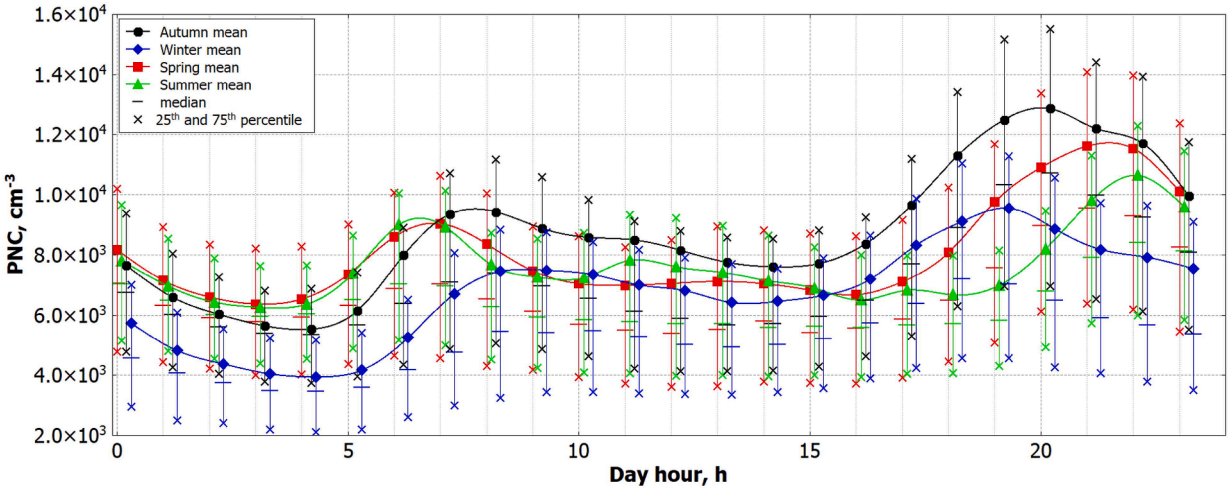

Fig. 4. The season segregated average hourly variation of PNC (as colored ○). Median and percentile (25th and 75th) values are shown as "–" and "", respectively. A slight shift in day hour was introduced for better visibility of measurement data. The separate station daily variation of PNC can be found in Figures S6 and S7.

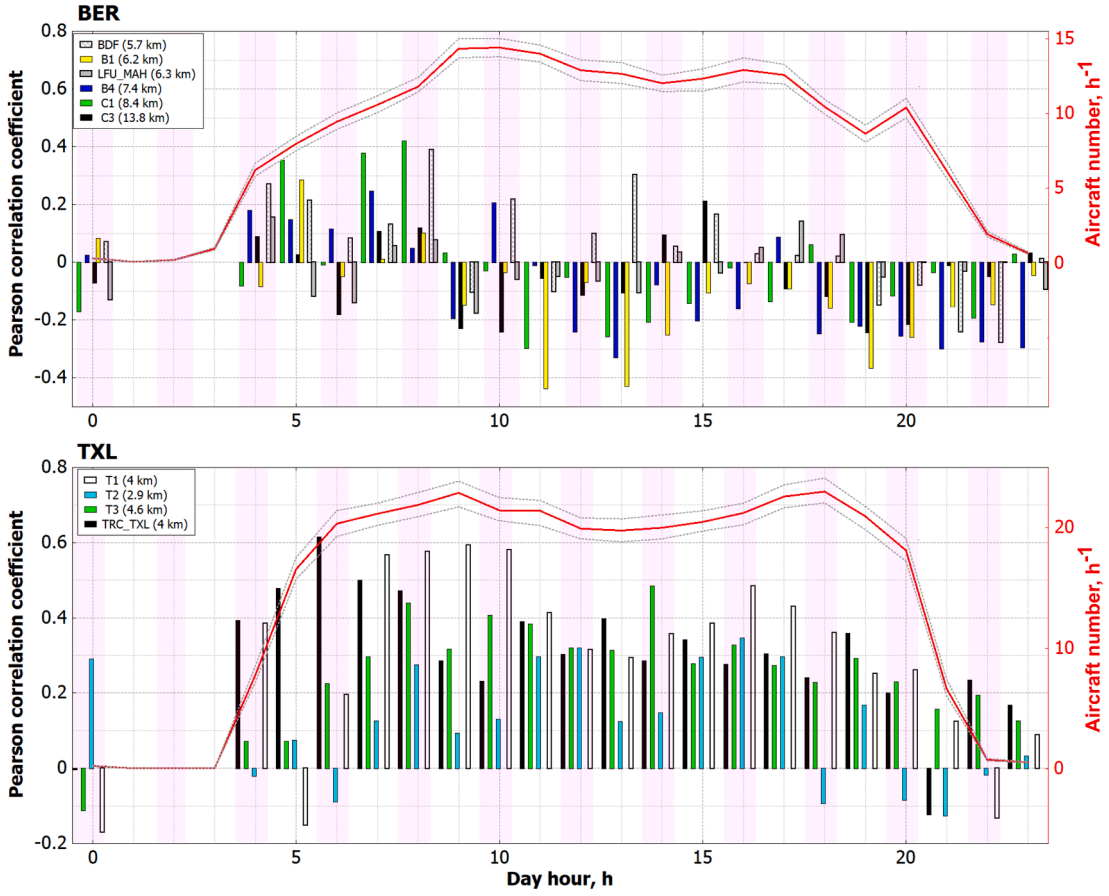

Fig. 5. An hourly variation of Pearson correlation coefficient between PNC at multiple measurement sites and air-traffic activity (as airplane number per hour, red line) at both BER (top) and TXL (bottom) airports. The measurement site distance to an airfield is shown in the legend. The pink shaded area is added for a better station separation between day hours. (For interpretation of the references to color in this figure legend, the reader is referred to the web version of this article.)

% of yearly PNC measurements were influenced by airport emissions (prevailing wind direction was from an airport sector, resulting in an elevated PNCs). Furthermore, as shown by Seidler et al. (2023), wind direction analysis alone cannot eliminate non-airport-related influence on PNC if there are other sources of pollutants between the measurement site and an airport (e.g., industrial facilities, major highways, residential areas, etc.). This poses a question – what is the real-world contribution (when not only the exemplary cases with air transport from the airport are considered) of airport emissions to PNC in the surrounding environments with increasing distance to an airfield. In the case of measurements in Berlin's north, measurements in the vicinity of TXL demonstrate a notably robust positive correlation between airport operations and PNC. Such an observation may suggest that PNC measurements in the vicinity of TXL airport bear the influence of air traffic,

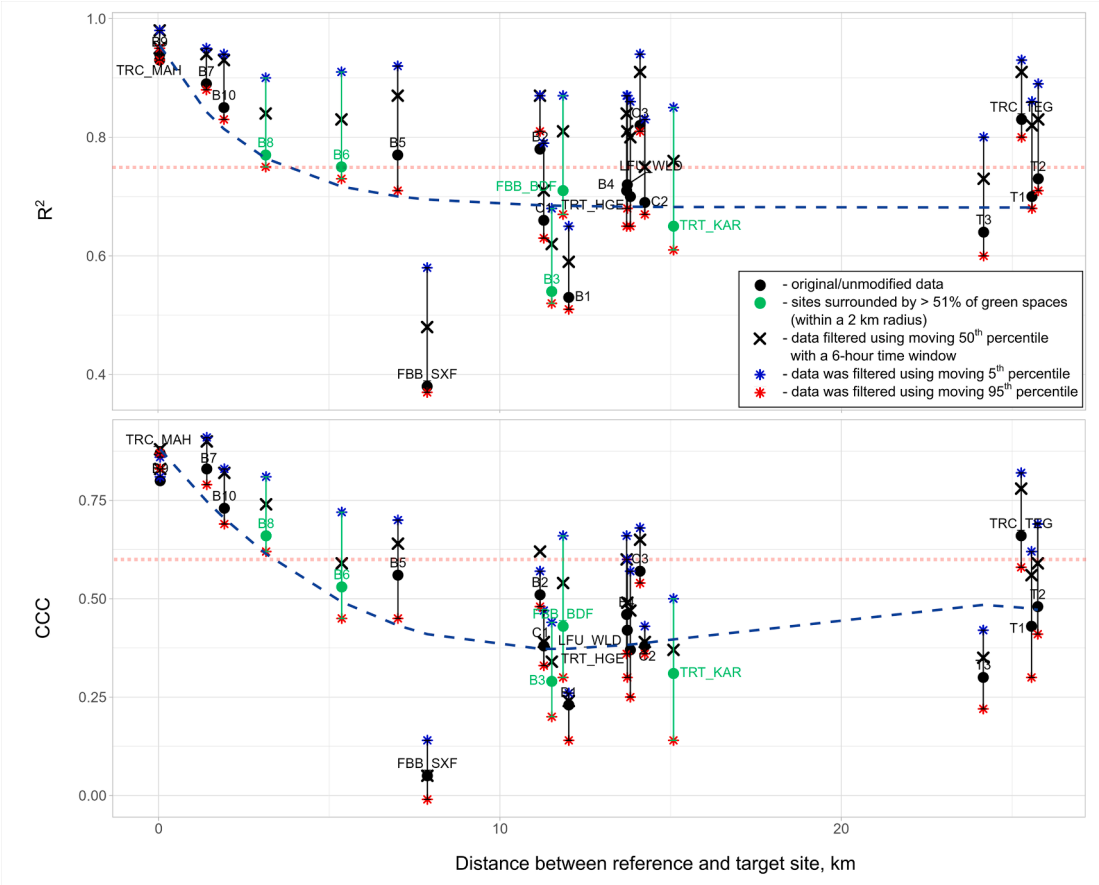

Fig. 6. The coefficient of determination (R^2) and concordance correlation coefficient (CCC) between PNC measurements at LFU MAH and all other measurement stations. The land use information was obtained from the CORINE CLC 2018 database. The reference site LFU MAH itself falls in this category with surrounding green spaces being > 55 %. The dashed regression line is used to visually emphasize the overarching trend within the data. The horizontal red lines delineate a threshold value, used as a basis for assessing the level of agreement across multiple sites. The statistical parameters are based on one-hour time resolution. (For interpretation of the references to color in this figure legend, the reader is referred to the web version of this article.)

or it may reflect a convergence of road-traffic activities and emissions with airport operations, engendering a spurious correlation between the observed PNC and the number of plane movements. In a study by Stacey et al. (2020), authors have shown that PNC at London airport fits within the range of traffic and urban background locations, if the PNSD is not considered. The problem of misinterpretation of airport and road traffic emissions can be illustrated as follows. In a study by Tremper et al. (2022), authors showed the fingerprint of air-traffic-related emissions as aerosol particles with a mobility diameter of approx. 20 nm. Aerosol particles in an urban environment have an average condensational growth rate of 3–11 nm h^{-1} (Jorga et al., 2023). With an average wind speed of 7.0 ± 4.2 km h^{-1} (an overall average ± standard deviation taken from the LFU MAH measurement site) and an average measurement site distance from an airport being approx. 7 km, the change in particle size would range from 3 to 10 nm. Such particle growth is enough to make air-traffic-related particles indistinguishable (in terms of their physical properties) from fresh traffic emissions, especially at a greater distance from an airfield. This underscores the critical significance of employing more advanced aerosol measurement instruments like mobility particle size spectrometer (MPSS, Seidler et al., 2023) and high-resolution mass spectrometry (HRMS, Ungeheuer et al., 2021), as well as data analysis techniques (e.g., positive matrix factorization) in providing a comprehensive picture of airport emissions influence on PNC at distances greater than 5 km from an airfield.

3.4. Comparing short-term-mobile versus long-term-fixed measurement sites

An important task of this work was to investigate how well long-term-fixed monitoring sites (including semi-mobile measurements) represent short-term measurements of PNC at multiple schools. This is important because of several reasons. Firstly, the PNC measurements at schools were conducted only briefly during the medical examination (Soppa et al., 2023), which limits the overview of PNC variation during different seasons. Secondly, long-term data is needed for source apportionment, segregating between road traffic- and air traffic-related pollutants, which will take place in later work. Furthermore, short-term measurement heavily reduces instances of capturing particles coming downwind from the airfields.

This study estimates the level of agreement between five long-term (operated for one year or more) monitoring sites—LFU MAH, LFU WLD, FFB BDF, FBB SXF, and TRC TXL—and various measurement sites at schools across Berlin (Fig. 1). It is expected that some school measurement sites will align more closely with nearby long-term monitoring stations due to shared influences from similar emission sources. Conversely, sites located further apart or in distinctly different environments (e.g., within an airport versus an urban setting) may exhibit notably different daily PNC patterns, leading to observable differences in their degree of agreement. As an example, we review the agreement between multiple measurement sites and the long-term monitoring site located west of BER airport (LFU_MAH). By focusing on the LFU_MAH site, we aim to demonstrate both the strengths and potential limitations

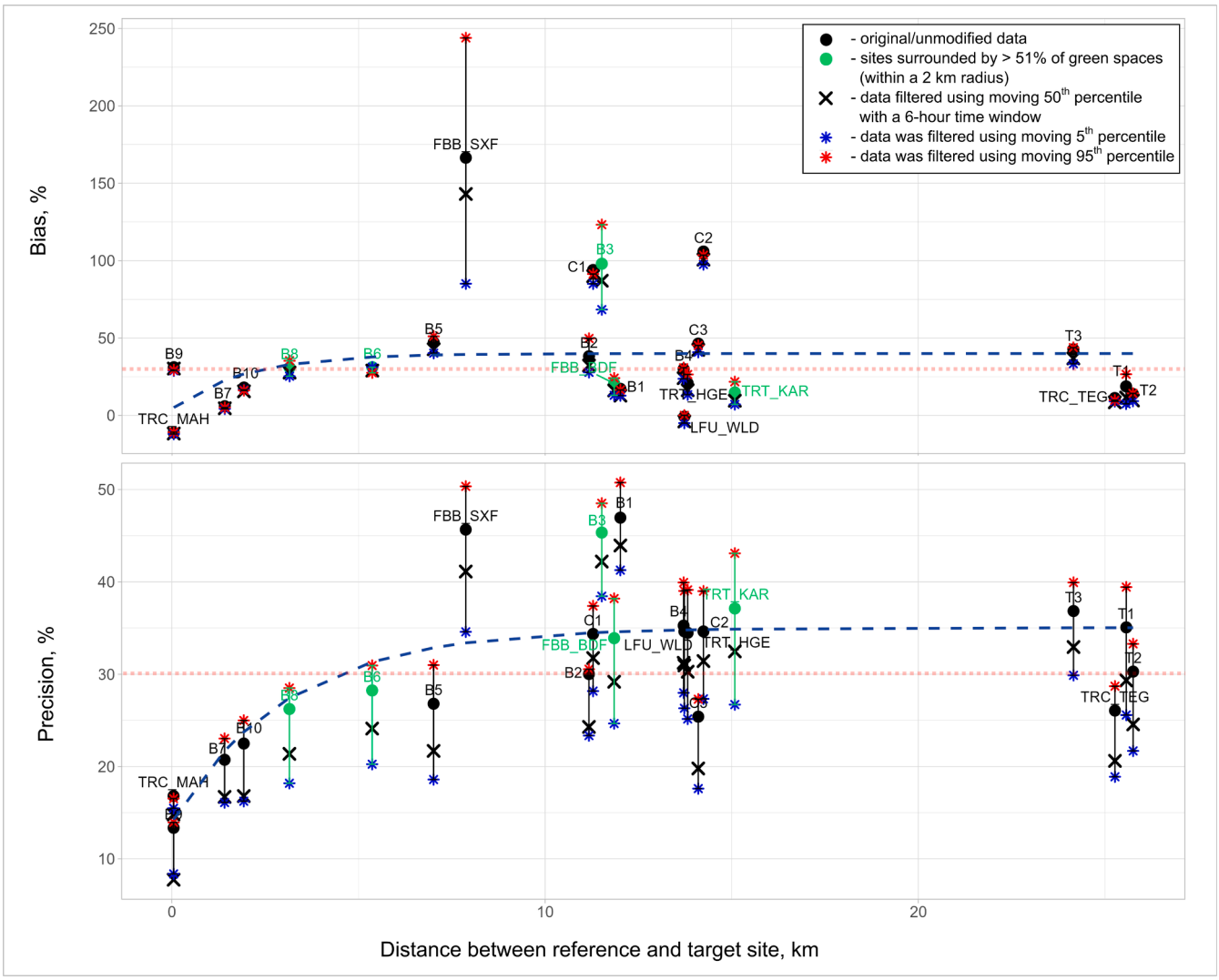

Fig. 7. The bias and precision between PNC measurements at LFU MAH and all other measurement stations. In the case of this study, higher values correspond to lower agreement between the measurement sites. The land use information was obtained from the CORINE CLC 2018 database. The reference site LFU MAH itself falls in this category with surrounding green spaces being > 55 %. The dashed regression line is used to visually emphasize the overarching trend within the data. The horizontal red lines delineate a threshold value, used as a basis for assessing the level of agreement across multiple sites. The statistical parameters are based on one-hour time resolution. In the case of this work, higher precision values show higher imprecision. (For interpretation of the references to color in this figure legend, the reader is referred to the web version of this article.)

of using long-term monitoring stations as reference points for evaluating the spatial variability and representativeness of air quality data collected at various school locations.

The statistical metrics used to evaluate the comparability of time-paired measurements between two sampling locations are shown in Fig. 6, Fig. S8 – S11, and Table S1. The agreement between PNC measured at the LFU MAH long-term measurement site and other short- and long-term sites is shown in Figs. 6 and 7. Initially, we will examine the PNC agreement between LFU MAH and the measurement sites nearest to the long-term sites, specifically B7 through B10. Based on R^2, CCC, precision, and bias metrics, the PNC measurements between short- and long-term measurement sites showed a good agreement, with the corresponding values of 0.86 ± 0.07, 0.76 ± 0.08, 21 ± 5 %, and 22 ± 12 %, respectively. When analyzing hourly, weekly, and monthly PNC at the sites mentioned (Fig. S12), a satisfactory agreement in PNC variation patterns was seen. The hourly PNC fluctuation at all measurement sites (LFU MAH, B7 – B10) showed an identical pattern of morning and evening road-traffic-related PNC increase. Such a good agreement between measured PNC values is likely to be attributed to the short distance between short- and long-term measurement sites (on average 1.6 ± 1.3 km) and the fact that all measurement sites are found in a homogeneous environment showing similar pollutant emission sources (e.g., traffic and residential heating). Based on the analysis presented in Fig. 6 (as well as SI), illustrating the degree of agreement between short-term and long-term measurement locations, usually a noticeable decline in agreement between short-term and long-term assessments of PNC occurs as the distance between measurement sites increases. In the case of the LFU MAH site (and based on the limits of our comparability metrics), the threshold distance between sites when the agreement between measured PNCs becomes unacceptable appears to be approx. 5 km.

As an illustration, the agreement in the measured PNC between the LFU MAH and TRC TXL sites adheres to the predefined criteria for agreement parameters. It can be categorized as strong ($R^2 = 0.83$, CCC = 0.66, precision = 26 %, and bias = 11 %), even when considering that these measurement locations are 25 km apart. Furthermore, after the 5 km distance mark, there seems to be no more decrease in agreement between the two measurement sites. In other words, independently of how far two stations are separated, there is always some degree of

agreement between two monitoring sites measuring PNC. This can be expected because in the urban environment, due to the synchronous nature of human activities (e.g., traffic-related rush hours, evening increase of PNC due to residential heating), as well as meteorological effects (boundary layer development and turbulent mixing during daytime) the PNC measured across the city most likely will experience some degree of similarity.

The opposite can be said about the agreement between measurement sites influenced by different emission sources. For example, the FBB SXF long-term measurement site is located inside the BER airport and showed a distinctly lower agreement to PNC measured at LFU MAH despite being less than 10 km away (Figs. 6 and 7). This is also true when comparing PNC measured at FBB SXF versus all short- and long-term monitoring sites (see Fig. S11). The metrics describing the agreement between measured PNC showed values CCC < 0.4, showing only poor agreement, even though R^2 in most cases was high. In fact, if R^2 would be the only metric used to judge how well short-term measurement sites across Berlin are represented by long-term monitoring sites, the agreement between FBB SXF and the majority (16 out of 20) of measurement sites could be termed as moderate or higher (based on correlation suggestions by BMJ (2021), $R^2 > 0.4$). Only by introducing other metrics (CCC, precision, and bias), can we gain more insights on how well the PNC measurements can be represented across the city. It is obvious that the FBB SXF long-term measurement site is highly affected by air traffic and airport-related emissions due to its proximity to the airfield. The low values of CCC are a result of decreased precision when comparing FBB SXF to other measurement sites that are further away from an airfield. From the perspective of hourly, daily, and monthly PNC variation, when comparing FBB SXF and other measurement sites, both PNC levels (FBB SXF PNC is up to 40 % higher compared to other measurement sites) and patterns are noticeably different, resulting in decreased precision and thus lower CCC values. We suggest that some agreement (CCC above 0.2) between the measurement sites and FBB SXF could be explained by coinciding air- and road-traffic activity patterns (see Fig. 5), as well as surrounding traffic-related emissions (including those from the airport supporting vehicles), which are transported to FBB SXF measurement site.

The previously discussed agreement between measurement sites was based on an unmodified PNC data set. Besides this, it is also interesting to investigate how the agreement would change if the measurement data were filtered using sliding percentile. A similar PNC data treatment was applied in earlier work (e.g., Kivekäs et al., 2014; Kecorius et al., 2019), where authors used sliding percentile function to either clean measurement data from local pollution or to reveal the background PNC variation. By tuning the 5th or 25th sliding percentile window size (in our case, we used 6 h), it is possible to extract background PNC variation, which is less influenced by local emissions. The opposite effect that highlights the effects of local emissions can be achieved by applying the 75th or 95th sliding percentile. The agreement between short- and long-term measurement sites with applied sliding percentile (5th, 50th, and 95th) can be seen in Figs. 6 and 7 (identified as red and blue asterisks). In general, after applying the sliding 5th percentile filter, the R^2, CCC, and precision metric values improved towards the sign of particularly good agreement between the two measurement sites. This is related to less variability in background PNCs, which is decided by factors influencing PNC on a regional scale (e.g., meteorology, long-range transport, seasonal variations). Although the overall agreement between sites has increased, the variability of the degree of agreement and how it depends on the distance to the measurement site remained. For example, for short-term measurement sites B1, B3, as well as long-term measurement site FBB SXF, the agreement with PNC measured at LFU MAH remained poor. This could be partly explained by the existence of micro-environments, where elevated background PNCs are the result of more homogeneous local emissions, which do not show as sudden pollutant concentration peaks but rather diluted and well-mixed elevated background PNCs (e.g., airport emissions or residential heating emissions during winter months in private housing communities). The opposite effect can be noticed when PNC data is filtered using the 95th sliding percentile. For the sites with initially good agreement (B9 – B10), accounting for more local sources did not have a negative effect on the PNC agreement. In this scenario, it is justifiable to assert with a reasonable level of confidence that the PNC measurements obtained at LFU MAH exhibit a strong agreement with measurement sites situated within a 5-kilometer radius, considering both background and local emissions, thus showing a favorable level of concordance. Lastly, no discernible effects on the concordance of measured PNCs were seen when measurement sites were categorized by their respective geographical areas. Sites falling within the classification of “green area” (including more than 51 % land cover within a 2-kilometer radius, as determined from the Coordination of Information on the Environment Land Cover database) are visually denoted by green color in Figs. 6 and 7. Notably, despite LFU MAH itself being situated within an area meeting the “green area” criteria (with over 55 % green land cover within the 2-kilometer radius), our findings show that sites sharing similar land cover attributes do not consistently exhibit a better agreement in measured PNC values. The comparison of PNC across other short- and long-term measurement sites can be found in SI (Fig. S8 – S11).

It is important to note that using PNC alone in long-term and short-term site comparisons may have limitations. The satisfactory agreement between PNCs does not necessarily mean an automatic agreement between other physical–chemical properties of pollutants. For example, if the PNCs agree well between the long-term measurement site and the site at one of the schools, the agreement between BC values or gaseous pollutants at those sites may not be as good. Moreover, the current state of scientific understanding does not provide insight into whether source apportionment outcomes are transferable between different measurement sites and, if so, to what extent this transferability is possible. Nevertheless, it is plausible to infer that if highly fluctuating PNC within an urban setting (Saha et al., 2019) shows a degree of agreement across two distinct sites, it is reasonable to expect that similar comparability may extend to other parameters, such as PNSD (as PNC is derivable from PNSD) or particle mass (mainly because of lower variability). The assumption here would be that particle physical–chemical properties are driven by similar sources (road traffic-related emissions, new particle formation, residential heating, etc.). To illustrate this, we calculated the mean PNSD between sites equipped with MPSS and the size-segregated Pearson correlation coefficient (Fig. S13). We observed that for particle number concentrations between 30 and 500 nm, the correlation coefficient was > 0.4, indicating an above-moderate PNSD agreement between the two measurement sites.

3.5. Number fractions of ultrafine particles

Multiple studies investigating airport influence into elevated PNC have used the term ultrafine particles (UFP), while no particle size information was measured (Hsu et al., 2014; Stafoggia et al., 2016; Yang et al., 2020; Fritz et al., 2022). Reporting UFP number concentration in such a manner may be misleading, as UFP refers to aerosol particles in the size range < 100 nm (preferably also indicating the lower size limit either determined by MPSS system or the lower detection limit of the CPC). It is true that in certain situations, PNC measurements may serve as a good proxy for UFP. Such examples include urban environments with prominent road-traffic emissions (e.g., Hussein et al., 2004; Rose et al., 2021), airports (e.g., Tremper et al., 2022; Trebs et al., 2023), as well as first hours of new particle formation (before particles grow to accumulation mode). In this work, measurements using MPSS at TRC TXL, TRC MAH, TRT KAR, and TRT HGE performed by TROPOS, as well as at BDF, performed by FBB allowed us to investigate the variation of UFP number fraction (UFP-nf) and how it depends on the distance to the airfield (without segregating between air coming from an airport and other directions). The UFP-nf data is shown in Fig. 8.

The overall measurement campaign mean ± standard deviation (median, 25th and 75th percentiles) of UFP-nf in herein mentioned measurement sites were UFP-$nf_{TRC\ TXL}$ = 0.83 ± 0.1 (0.84, 0.77, 0.9), UFP-$nf_{TRC\ MAH}$ = 0.83 ± 0.1 (0.85, 0.77, 0.9), UFP-$nf_{TRT\ KAR}$ = 0.8 ± 0.12 (0.82, 0.73, 0.9), UFP-$nf_{TRT\ HGE}$ = 0.81 ± 0.12 (0.84, 0.74, 0.91), and UFP-$nf_{FBB\ BDF}$ = 0.81 ± 0.11 (0.83, 0.74, 0.9). As it can be seen, the average UFP-nf at several measurement sites in Berlin is constant with a value of approx. 0.8 (UFP contributes approx. 80 % of measured PNC). Seasonal UFP-nf varied from an average value of 0.8 ± 0.1 (0.82, 0.73, 0.9) in summer and winter months, to an average of 0.84 ± 0.1 (0.85, 0.78, 0.92) in spring and autumn. The highest median (25th and 75th percentiles) UFP-nf values were seen in spring, and were 0.87 (0.79, 0.92). One probable reason for higher UFP-nf during spring months could be intensified occasion of new particle formation, which is known to produce high numbers of ultrafine particles (Nieminen et al., 2018; Sulo et al., 2021). With respect to UFP-nf dependence on the distance to an airport, one would expect to see the highest UFP-nf at a distance closest to the airfield. This is because of lesser dilution and the fact that the aerosol particle emissions from the airplanes are in a size range of 4–100 nm (Mazaheri et al., 2009; Tremper et al., 2022). The smallest particle size fractions may be a result of new particle formation facilitated by jet oil (Ungeheuer et al., 2022), while the bigger particles are emitted directly from the combustion process (Rogers et al., 2005). In the case of Berlin, there is a slight decrease in UFP-nf with respect to the distance to an airfield (except in winter months). However, the change is slow – from 1 % to 2 % decrease in UFP-nf km^{-1}. It is also not obvious that the observed minor differences in UFP-nf between different sites with various distances to an airfield are the result of plane-related emissions. For example, the TRT KAR site is found furthest away from the airfield. However, lower UFP-nf may be a mixed result of weaker UFP emissions and secondary aerosol mass production during summer, as well as residential heating during colder months, which both increase the number of accumulation mode aerosol particles (lowering UFP-nf). The latter is especially true for TRC TXL and FBB BDF measurement sites, which, although found closest to an airfield, are also surrounded by densely populated residential areas. In winter months, both the TRC TXL and FBB BDF showed lower UFP-nf values than sites further away from an airfield. It must be noted, however, that PNC data available from the TRC TXL measurement site does not fully cover winter months with high TXL airport activity,represents the situation when TXL airport was decommissioned, and the lower observed UFP-nf during winter months at TRC TXL may be a result of decreased air-traffic intensity.

The hourly variation of UFP-nf can be seen in Fig. S14. During all seasons, the lowest average UFP-nf was observed between midnight and 6 AM and was between approx. 0.75 (in winter) and 0.8 (in spring). From 6 to 7 AM, the UFP-nf gradually increased and reached its maximum value between approx. 0.83 (in winter) to 0.9 (in spring) between 6 and 11 PM. A slight dip in UFP-nf between midnight and 6 AM can be explained by a decreased emission of UFP into the atmosphere, and vice versa – an increase in UFP-nf during working hours suggests an accumulation of UFP in the atmosphere, which can primarily be linked to road-traffic. An interesting pattern of UFP-nf appeared during summer when UFP-nf remained stable (approx. 0.8) between 6 AM and 6 PM. This may show an efficient secondary aerosol production in the atmosphere (Saha et al., 2018), which balances out the emissions of UFP, supporting stable UFP-nf. Compared to earlier studies, Asmi et al. (2011) and Rose et al. (2021) reported on average slightly lower (0.73 ± 0.07; calculated from data supplied both in the publications, as well as supplementary information) UFP-nf from many central Europe and urban measurement sites, respectively. Marginally lower UFP-nf might be a result of the smaller size range used by the authors (20 – 500 nm, compared to 10 – 800 nm in this study), as PNSD in both publications shows a steep decrease in PNC > 500 nm and a constantly high PNC > 20 nm.

3.6. COVID-19, airport closure/opening influence on PNC and UFP-nf

As mentioned in Section 2.2, several instances occurred during the measurement period when airport activity changed from high to low and vice versa. Such events were caused by a TXL closure, BER opening, and the COVID-19 pandemic. It allowed us to investigate how changes in air traffic affect PNC and UFP-nf in the surrounding environments. Moreover, decreased plane activity shall provide a PNC reference (PNC influenced by all other particle sources but air traffic). It is important to note that our discussion here pertains to overall changes in PNC, without consideration of wind direction. The justification for this approach lies in the premise that if air traffic serves as a significant source of UFP, its impact on particle PNC should be discernible when averaged over an extended period. The PNC in several measurement sites during the previously mentioned time periods is given in Table 2.

During the whole measurement period analyzed in this work, only one site (T1) was operated during the four distinct phases of varying airport activity in the vicinity of TXL. As can be seen from Table 2, the average PNC at the T1 measurement site during the high airport activity was 15400 ± 13300 cm^{-3}, which is almost two-fold higher than the PNC during the measurement period after airport closure. During the COVID-19 pandemic, airport activity reduction by 10-fold resulted only in a 35 % reduction in PNC. Furthermore, after the COVID-19 pandemic restrictions on air traffic were lifted, the measured PNC in the vicinity of TXL airport has not changed (despite four times increase in air traffic).

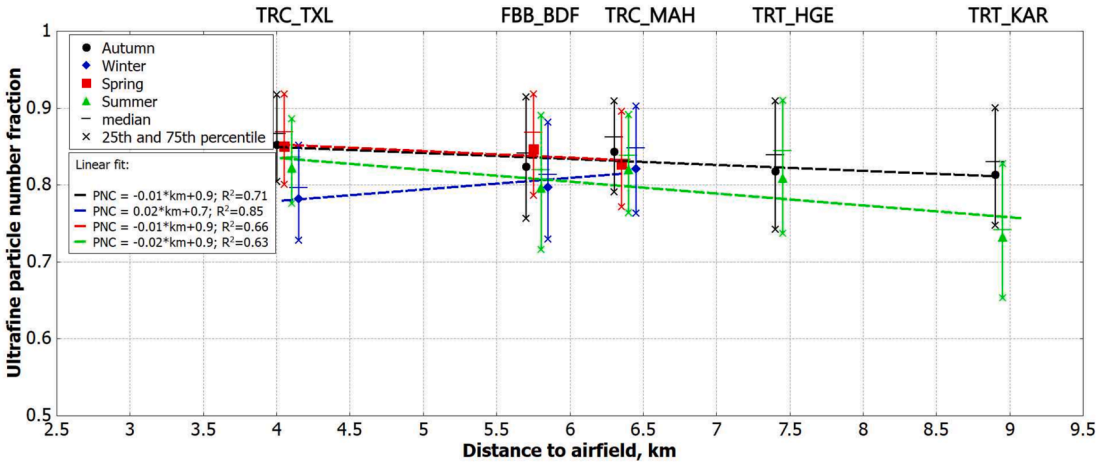

Fig. 8. Ultrafine particle number fraction (UFP-nf) segregated by season and distance to an airfield. A slight shift in distance between sites is introduced for better visibility.

Table 2
PNC in several measurement sites during time periods, which affected airport activity. The PNC values are given as mean ± standard deviation (median). The airport activity "ξ is presented by take-off and landing plane numbers per day (retrieved from airport traffic statistics, available online at https://corporate.berlin-airport.de/, accessed: October 19, 2023).

TXL				
Site	PNC prior to COVID-19, before TXL closure ξ = 190	PNC during COVID-19, before TXL closure ξ = 19	PNC after COVID-19, before TXL closure ξ = 86	PNC after TXL closure, ξ = 0
T1	15400 ± 13300 (10100)	9900 ± 2700 (9200)	10000 ± 6000 (8400)	7900 ± 4700 (6800)
TRC TXL	No data	No data	7500 ± 4400 (6300)	5600 ± 3500 (4800)
T3	No data	No data	11800 ± 8000 (10100)	7300 ± 4200 (6400)
T2	No data	No data	9700 ± 5900 (8100)	6500 ± 3600 (5700)
BER				
Site	PNC before BER opening, before COVID-19, ξ = 92	PNC during COVID-19, before BER opening, ξ = 21	PNC before BER opening, after COVID-19, ξ = 58	PNC after BER opening, ξ = 168/day
LFU MAH	No data	7300 ± 4400 (6300)	7100 ± 4000 (6200)	6700 ± 4700 (5500)
B1	11500 ± 8200 (9000)	No data	No data	7300 ± 6300 (5600)
C1	8800 ± 4900 (7800)	No data	No data	7300 ± 4900 (6200)

The reason for this could be related to the specifics of airport activity during the COVID-19 pandemic and meteorological conditions. By investigating the reports on the airport traffic statistics, we saw that airport-related activities did not stop completely (e.g., cargo transportation continued to support the global supply chain) during the COVID-19 pandemic. This means that although airplane numbers decreased, the supporting airport infrastructure had to remain operational, which may have caused a diminished reduction in PNC when comparing COVID-19 and post-COVID-19 PNC versus PNC after the TXL closure. This can be supported to a degree by Tremper et al. (2022), as well as Masiol et al. (2016), who found that not only plane engine emissions contribute to PNC related to airports. An overall PNC decrease at measurement sites found around TXL was 30 % when comparing post-COVID-19 airport operation and time after TXL closure. Although the direct comparison is not applicable, our observed airport contribution to PNC is noticeably higher than that (17 %) reported by Tremper et al. (2022). Masiol et al. (2017) noted that the airport contributes approx. 32–33 % to PNC in airport surrounding areas, which closely matches our observations. After the TXL closure, the UFP-nf decreased only marginally (from approx. 0.86 to 0.81), which may suggest that the reduction in PNC observed after TXL closure was related to a reduction of particles emitted from similar sources (e.g., road traffic and not the plane engines). The opposite situation was seen at measurement sites found around BER. On average, PNC during low airport activity (before BER airport was opened) was approx. 20 % higher compared to those after the BER went into operation. However, it must be noted that high concentrations reported from the B1 measurement site may have been influenced by either road-traffic and/or a new particle formation, contributing significantly to PNC. This is because, during low-flight activity, the PNC measurements at the B1 site were conducted in spring and winter, with a mean PNC of 11,800 and 9300 cm^{-3}, respectively. It is therefore important to look at how NPF events may influence PNC and UFP levels.

3.7. New particle formation influence onto PNC and UFP-nf

The measurements of PNSD at several sites (operated by TROPOS and FBB) allowed us to observe and investigate the regional NPF effect on UFP number concentrations and UFP-nf. During the whole measurement period, a total of 96 days with regional NPF events were found (NPF with a characteristic banana shape particle growth; Ström et al., 2009; Kulmala et al., 2012). All regional NPF events were identified manually through visual inspection of daily PNSD contour plots. An exemplary case of NPF is shown in Fig. S15. During the beginning of NPF, a vast number of sub-10 nm particles is created, substantially increasing UFP-nf, which gradually decreases as particles grow beyond 100 nm. When the newly created particles grow from nucleation (particle diameters from 2 to 20 nm) to accumulation mode (> 100 nm), they can be mistakenly classified as plane emissions (if no other physical–chemical information besides PNC is known). It is worth noting that here, we are talking about regional new particle formation, with a distinct feature of subsequent particle growth, which shows that newly formed particles are not the result of plane emissions. Although Ungeheuer et al. (2022) have shown that jet oil nucleation is an important mechanism contributing to ultrafine particle number concentration near airports, these particles are formed fast close to the point of emission and are unlikely to grow uniformly, forming a banana-shaped pattern in PNSD. Without an abrupt change in air mass (which could interrupt regional NPF and present itself as irregularity in PNSD, which can be mistaken for airport emissions), it is simple to distinguish between local (plane influence) versus regional (no plane influence) NPF events. While it is evident that UFPs from the jet engine-induced NPF shall be included in exposure assessment studies, the UFP from regional NPF ideally should be separated. It is worth mentioning that to this date, no studies exist investigating regional NPF effects on human health, despite such events regionally producing UFP number concentrations matching and sometimes exceeding those of air- and road traffic.

The NPF effect on UFP number concentration and UFP-nf is shown in Fig. 9. In the period from midday to 3 PM, the mean value ± standard deviation of UFP number concentration during non-NPF days was 4200 ± 780 cm^{-3} (with a UFP-nf of 0.82 ± 0.01). Taking NPF into account, the UFP number concentration increased to 7400 ± 1700 cm^{-3} (with a UFP-nf to PNC of 0.89 ± 0.01) during the same period of the day. During the NPF events, the concentration of UFP particles in the airport surrounding measurement sites increased by 1.8 times compared to days (from midday to 3 PM) without the NPF. The hourly PNC variation for different sites during days with and without regional new particle formation events is shown in Fig. S16. As previously mentioned, and observed in previous studies (e.g., Kulmala et al., 2012), the NPF influence on PNC is mostly visible during midday hours, when nucleation occurs, producing high numbers of ultrafine particles. The overall mean contribution of NPF onto PNC (based on daily concentration means) was 15 % (6520 2360 during non-NPF days versus 7650 2330 during NPF event days). On days with NPF, the PNC can be expected to be 15 % higher compared to non-NPF days. The probability density functions of PNC during NPF and non-NPF days are shown in Fig. S17.

This may pose a question if people's exposure to UFPs originating from the regional NPF is more frequent (due to particles being created over a large area) than to plane-related pollutants (which require specific meteorological conditions (e.g., wind patterns) to be transported to residential areas). In a study by Seidler et al. (2023), authors showed that depending on the measurement site location, the instances when the

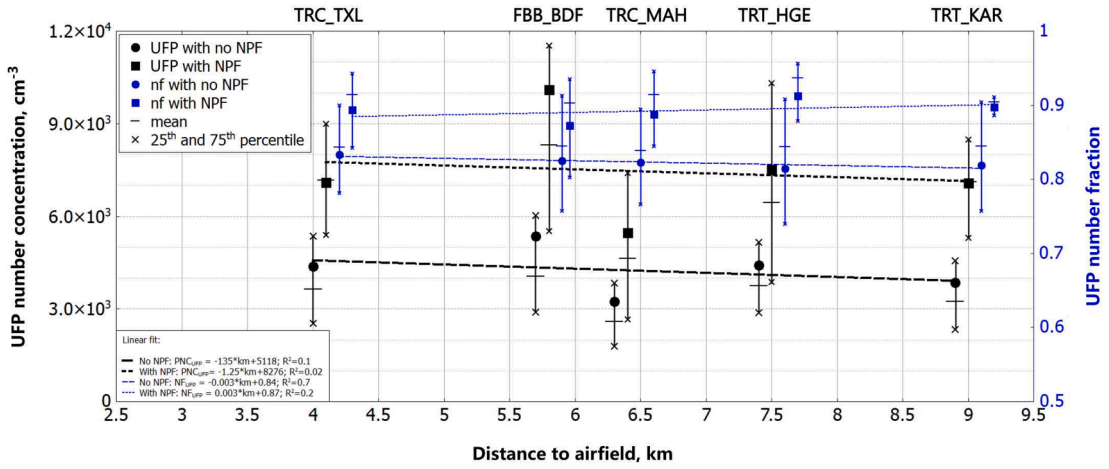

Fig. 9. Regional NPF influences UFP number concentration and UFP-nf measured in the vicinity of TXL and BER airports. The data was filtered to include solely the time periods between midday and 3 PM (highlighting the effect of NPF on UFP number concentration and UFP-nf). Please note that the results from TRC TXL cover high and low TXL airport activities, while the rest of the sites (found around BER airport) represent only high airport activity.

air is coming from an airport may be low (10 to 14 %). f the airport is found outside of densely populated areas, it may be that due to meteorological conditions and pollutant dilution the airport related exposure to UFPs, at several kilometers from the airport, is minimal. Meanwhile, in the case of regional NPF, it would certainly mean that a greater population would be exposed to high concentrations of UFPs despite meteorological conditions. While the health effects of regional NPF are still unknown, we show that it is important to account for nucleation events when investigating PNC in relation to road- and air traffic emissions.

4. Summary and conclusion

In this study, we conducted a multifaceted analysis, which encompassed a) investigating the spatial and temporal variability of the total aerosol particle number concentration (PNC) at multiple locations surrounding two international airports in Berlin and Brandenburg, Germany; b) assessing the relationship between PNC measurements obtained from short-term, multiple locations and those from long-term, fixed monitoring sites; c) examining the factors that contribute to the determination of the ultrafine particle number concentration and number fraction (UFP-nf). The data collection efforts involved measuring PNC and ground-level meteorological parameters at 16 schools located at varying distances (ranging from 3 to 14 km) from TXL and BER airports and in control areas. In addition to the PNC measurements at schools, we used a dataset on PNC and PNSD produced by the ULTRAFLEB consortium. Also, continuous long-term PNC data was sourced from the LfU.

The average PNC for Berlin, calculated from all measurement sites and periods, was 7900 ± 7000 cm^{-3}. The median PNC value was approximately 6200 cm^{-3}, and the 25th/75th percentile ranged from 4100 cm^{-3} to 9500 cm^{-3}. These values are consistent with those found in other European cities. The highest median seasonal PNC concentration in Berlin was in spring at around 6700 cm^{-3}, followed by autumn (6500 cm^{-3}) and summer (6300 cm^{-3}), with the lowest in winter (5100 cm^{-3}). Most measurement sites generally showed only limited PNC seasonal variability, determined by traffic-related emissions, which have stable seasonal patterns. The highest PNCs were recorded in spring, highlighting the influence of secondary aerosol processes like new particle formation (NPF), which can be a significant source of particles in urban environments.

Measurements at multiple locations with varying distances to airfields show a decrease in PNC as the distance from the airfield increases. PNC decreased from an average value of 16500 cm^{-3} (measured within the airport) to 8000 cm^{-3} at 5 km. Seasonal variations in PNC and the distance to an airfield were notable, with influencing factors such as residential heating in winter and NPF in spring. Long-term monitoring data covering all seasons revealed a slight decrease in PNC of approx. 145 cm^{-3} km^{-1}.

Under a critical examination of the comparability between short-term mobile measurements and long-term fixed monitoring sites, a good agreement was observed when the two sites were within 5 km distance. The agreement declined as the distance between measurement sites increased, especially when different emission sources influenced the sites. Notably, measurements taken inside the airport at FBB SXF showed a distinctly lower agreement with measurement sites further away, reflecting the impact of air traffic and airport-related emissions. Several instances were seen when measurements of PNC show good agreement across the city, even at large distances (approx. 25 km). This can be explained by the synchronous nature of human activities and meteorological effects.

Analysis of PNSDs at several measurement sites in Berlin revealed that the UFP-nf was constant, with an average of around 0.8. Seasonal variations showed the average UFP-nf in summer and winter months is approximately 0.8 ± 0.1 (median: 0.82, 25th percentile: 0.73, 75th percentile: 0.9). In spring and autumn, the UFP-nf values were slightly higher, averaging around 0.84 ± 0.1 (median: 0.85, 25th percentile: 0.78, 75th percentile: 0.92). The higher UFP-nf values during spring were related to NPF events. Regarding the relationship between UFP-nf and the distance from the airport, there was a gradual change in UFP-nf, with a decrease of 1 to 2 % per kilometer. However, the variations in UFP-nf between sites at different distances from the airport were relatively minor.

In the context of the impact of airport closure (TXL) and inauguration (BER), alongside the COVID-19 pandemic, we saw that during periods of high airport activity, particularly before the closure of TXL, the PNC levels at the T1 measurement site were noticeably elevated, with an average of approx. 15400 ± 13300 cm^{-3}. Air traffic restrictions due to the COVID-19 pandemic led to a tenfold reduction in airport activity, resulting in a 35 % decrease in PNC. After the pandemic-related restrictions were lifted and airport activity resumed (although not to the degree seen before), PNC levels near TXL did not significantly change despite a fourfold increase in air traffic, which can be attributed to certain airport-related activities, like cargo transportation. Furthermore, it was noted that after the closure of TXL, UFP-nf experienced only a marginal decrease, suggesting that the reduction in PNC was primarily associated with a decrease in particles from sources other than plane engines, e.g., road traffic emissions and new particle formation.

The analysis of the influence of NPF on PNC and UFP-nf revealed that during NPF event days, the number concentration of UFP particles at airport-adjacent measurement sites increased by 1.8 times compared to days without NPF events. While the health implications of UFP from NPF remain unknown, this study underscores the importance of considering nucleation events when investigating PNC in relation to road and air traffic emissions.

This study contributes valuable insights into PNC variations, their seasonal patterns, and their relation to airports and local sources in Berlin. It underscores the significance of continuous, long-term measurements for accurate assessment and the complex interplay of factors shaping PNC levels in urban environments. These findings will be used in subsequent health-assessment studies.

CRediT authorship contribution statement

Simonas Kecorius: Writing – review & editing, Writing – original draft, Visualization, Validation, Methodology, Investigation, Formal analysis, Data curation, Conceptualization. **Susanne Sues:** Writing – review & editing, Validation, Investigation, Data curation. **Leizel Madueño:** Writing – review & editing, Visualization, Validation, Software, Investigation. **Alfred Wiedensohler:** Writing – review & editing, Supervision, Project administration, Funding acquisition. **Ulf Winkler:** Writing – review & editing, Validation, Investigation, Data curation. **Andreas Held:** Writing – review & editing. **Sabine Lüchtrath:** Writing – review & editing, Validation, Investigation, Data curation. **David C. Beddows:** Writing – review & editing, Visualization, Validation, Software, Investigation. **Roy M. Harrison:** Writing – review & editing, Visualization, Validation, Software, Investigation. **Mario Lovric:** Writing – review & editing, Visualization, Validation, Software, Investigation. **Vanessa Soppa:** Writing – review & editing. **Barbara Hoffmann:** Writing – review & editing, Supervision, Project administration, Funding acquisition. **Miriam Wiese-Posselt:** Writing – review & editing, Supervision, Project administration, Funding acquisition. **Andreas Kerschbaumer:** Writing – review & editing. **Josef Cyrys:** Writing – review & editing, Supervision, Project administration, Funding acquisition.

Declaration of competing interest

The authors declare that they have no known competing financial interests or personal relationships that could have appeared to influence the work reported in this paper.

Acknowledgments

The BEAR study is funded by the German Research Council (HO 3314/13-1, WI 5556/2-1, CY 68/5-1). The air pollution modeling in this project is part of the project “Ultrafeinstaubbelastung durch Flughäfen in Berlin” (ULTRAFLEB) project and funded by the German Federal Environment Agency (Umweltbundesamt; FKZ 3720522010; AZ. 54 551/4). BEAR also received financial support from municipalities in Brandenburg (Blankenfelde-Mahlow, Eichwalde, Schönefeld und Schulzendorf), the Ministry of Social Affairs, Health, Integration and Consumer Protection of the State of Brandenburg (MSGIV) and a donation from the association “Schutzgemeinschaft Umlandgemeinden Flughafen Schönefeld e.V. Mario Lovric acknowledges funding by the EU-Commission Grant Nr. 101057497 - EDIAQI. We gratefully acknowledge Ulf Janicke from Janicke Consulting, Überlingen, Germany, for generously providing flight activity patterns from TXL and BER airports. We acknowledge the aerosol measurement data obtained from Hannes Brauer and Lutz Schaefer (Landesamt für Umwelt Brandenburg, Potsdam) and Sebastian Aust (Flughafen Berlin Brandenburg GmbH, Berlin). We extend our sincere appreciation to the day care facilities, Berlin districts, Brandenburg municipalities, the Ministry of Social Affairs, Health, Integration and Consumer Protection of the State of Brandenburg, the Ministry of Agriculture, Environment and Climate Protection of the State of Brandenburg, and the Berlin Senate Administration for their invaluable support. Special recognition is due to Sven Klemer at the Technische Universität Berlin, Institute of Environmental Science and Technology, as well as Lukas Semenyuk, Benno Wolbring, and Simon Barchewitz at the Charité Berlin, Institute of Hygiene and Environmental Medicine, for their invaluable assistance with measurements; and particularly for the maintenance and relocation of the CPC devices. We would also like to thank Jennifer Golembus and Kerstin Theisen, study assistants at the Charité Berlin, Institute of Hygiene and Environmental Medicine, for planning the relocation of the CPC measuring devices from school to school.

Appendix A. Supplementary material

Supplementary data to this article can be found online at https://doi.org/10.1016/j.envint.2024.109086.

Data availability

The data used is freely available upon a reasonable request from the corresponding author.

References

Asmi, A., Wiedensohler, A., Laj, P., Fjaeraa, A.M., Sellegri, K., Birmili, W., Weingartner, E., Baltensperger, U., Zdimal, V., Zikova, N., Putaud, J.P., 2011. Number size distributions and seasonality of submicron particles in Europe 2008–2009. Atmos. Chem. Phys. 11 (11), 5505–5538.

Barlund, C.S., Carruthers, T.D., Waldner, C.L., Palmer, C.W., 2008. A comparison of diagnostic techniques for postpartum endometritis in dairy cattle. Theriogenology 69 (6), 714–723.

Bendtsen, K.M., Bengtsen, E., Saber, A.T., Vogel, U., 2021. A review of health effects associated with exposure to jet engine emissions in and around airports. Environ. Health 20 (1), 1–21.

BMJ, 2021. ’11. Correlation and regression’. https://www.bmj.com/about-bmj/resources-readers/publications/statistics-square-one/11-correlation-and-regression.

Brean, J., Rowell, A., Beddows, D.C., Weinhold, K., Mettke, P., Merkel, M., Tuch, T., Rissanen, M., Maso, M.D., Kumar, A., Barua, S., 2024. Road traffic emissions lead to much enhanced new particle formation through increased growth rates. Environ. Sci. Tech.

Camalier, L., Eberly, S., Miller, J. and Papp, M., 2007. Guideline on the meaning and use of precision and bias data required by 40 CFR Part 58, appendix A. EPA-454/B-07-001.

Carslaw, D.C., Ropkins, K., 2012. Openair – R package for air quality data analysis. Environ. Model. Softw. 27, 52–61.

Casquero-Vera, J.A., Lyamani, H., Titos, G., Moreira, G.D.A., Benavent-Oltra, J.A., Conte, M., Contini, D., Järvi, L., Olmo-Reyes, F.J., Alados-Arboledas, L., 2022. Aerosol number fluxes and concentrations over a southern European urban area. Atmos. Environ. 269, 118849.

Cheung, H.C., Chou, C.K., Huang, W.R., Tsai, C.Y., 2013. Characterization of ultrafine particle number concentration and new particle formation in an urban environment of Taipei, Taiwan. Atmos. Chem. Phys. 13 (17), 8935–8946.

Coelho, S., Ferreira, J., Rodrigues, V., Lopes, M., 2022. Source apportionment of air pollution in European urban areas: lessons from the ClairCity project. J. Environ. Manage. 320, 115899.

Considine, E.M., Reid, C.E., Ogletree, M.R., Dye, T., 2021. Improving accuracy of air pollution exposure measurements: statistical correction of a municipal low-cost airborne particulate matter sensor network. Environ. Pollut. 268, 115833.

Diener, A., Lucht, S., Lüchtrath, S., Glaubitz, L., Weinhold, K., Winkler, U., Wiedensohler, A., Cyrys, J., Gastmeier, P., Wiese Poselt, M. and Hoffmann, B., 2021, August. The Berlin-Brandenburg Air Study – a natural experiment investigating health effects from changes in airport-related exposures. In ISEE Conference Abstracts (Vol. 2021, No. 1).

Fritz, S., Grusdat, F., Sharkey, R., Schneider, C., 2022. Impact of airport operations and road traffic on the particle number concentration in the vicinity of a suburban airport. Front. Environ. Sci. p.1583.

Guo, S., Hu, M., Peng, J., Wu, Z., Zamora, M.L., Shang, D., Du, Z., Zheng, J., Fang, X., Tang, R., Wu, Y., 2020. Remarkable nucleation and growth of ultrafine particles from vehicular exhaust. Proc. Natl. Acad. Sci. 117 (7), 3427–3432.

HEI Review Panel on Ultrafine Particles, 2013. Understanding the Health Effects of Ambient Ultrafine Particles. HEI Perspectives 3. Health Effects Institute, Boston, MA.

Henseler, J., Ringle, C.M., Sinkovics, R.R., 2009. The use of partial least squares path modeling in international marketing. In New challenges to international marketing (Vol. 20, pp. 277-319). Emerald Group Publishing Limited.

Hsu, H.H., Adamkiewicz, G., Houseman, E.A., Spengler, J.D., Levy, J.I., 2014. Using mobile monitoring to characterize roadway and aircraft contributions to ultrafine particle concentrations near a mid-sized airport. Atmos. Environ. 89, 688–695.

Hudda, N., Simon, M.C., Zamore, W., Durant, J.L., 2018. Aviation-related impacts on ultrafine particle number concentrations outside and inside residences near an airport. Environ. Sci. Tech. 52 (4), 1765–1772.
Hudda, N., Durant, L.W., Fruin, S.A., Durant, J.L., 2020. Impacts of aviation emissions on near-airport residential air quality. Environ. Sci. Tech. 54 (14), 8580–8588.
Hussein, T., Puustinen, A., Aalto, P.P., Mäkelä, J.M., Hämeri, K., Kulmala, M., 2004. Urban aerosol number size distributions. Atmos. Chem. Phys. 4 (2), 391–411.
Janssen, N.A., Gerlofs-Nijland, M.E., Lanki, T., Salonen, R.O., Cassee, F., Hoek, G., Fischer, P., Brunekreef, B. and Krzyzanowski, M., 2012. Health effects of black carbon. World Health Organization. Regional Office for Europe.
Janssen, N.A.H., Hoekstra, J., Houthuijs, D., Jacobs, J., Nicolaie, A. and Strak, M., 2022. Effects of long-term exposure to ultrafine particles from aviation around Schiphol Airport. RIVM rapport 2022-0068 (2022). Available From: https://www.rivm.nl/bibliotheek/rapporten/2022-0068.pdf (Accessed August 10, 2024).
Jorga, S.D., Florou, K., Patoulias, D., Pandis, S.N., 2023. New particle formation and growth during summer in an urban environment: a dual chamber study. Atmos. Chem. Phys. 23 (1), 85–97.
Kecorius, S., Vogl, T., Paasonen, P., Lampilahti, J., Rothenberg, D., Wex, H., Zeppenfeld, S., van Pinxteren, M., Hartmann, M., Henning, S., Gong, X., 2019. New particle formation and its effect on cloud condensation nuclei abundance in the summer Arctic: a case study in the Fram Strait and Barents Sea. Atmos. Chem. Phys. 19 (22), 14339–14364.
Kennedy, I.M., 2007. The health effects of combustion-generated aerosols. Proc. Combust. Inst. 31 (2), 2757–2770.
Keuken, M.P., Moerman, M., Zandveld, P., Henzing, J.S., Hoek, G., 2015. Total and size-resolved particle number and black carbon concentrations in urban areas near Schiphol airport (the Netherlands). Atmos. Environ. 104, 132–142.
Kim, J., Lee, J.H., 2022. A novel graphical evaluation of agreement. BMC Med. Res. Method. 22 (1), 51.
Kivekäs, N., Massling, A., Grythe, H., Lange, R., Rusnak, V., Carreno, S., Skov, H., Swietlicki, E., Nguyen, Q.T., Glasius, M., Kristensson, A., 2014. Contribution of ship traffic to aerosol particle concentrations downwind of a major shipping lane. Atmos. Chem. Phys. 14 (16), 8255–8267.
Kulmala, M., Petäjä, T., Nieminen, T., Sipilä, M., Manninen, H.E., Lehtipalo, K., Dal Maso, M., Aalto, P.P., Junninen, H., Paasonen, P., Riipinen, I., 2012. Measurement of the nucleation of atmospheric aerosol particles. Nat. Protoc. 7 (9), 1651–1667.
Lammers, A., Janssen, N.A.H., Boere, A.J.F., Berger, M., Longo, C., Vijverberg, S.J.H., Neerincx, A.H., Maitland-Van der Zee, A.H., Cassee, F.R., 2020. Effects of short-term exposures to ultrafine particles near an airport in healthy subjects. Environ. Int. 141, 105779.
Lin, L.I., 1989. A concordance correlation coefficient to evaluate reproducibility. Biometrics, 45(1), 255–268. https://www.ncbi.nlm.nih.gov/pubmed/2720055.
Masiol, M., Vu, T.V., Beddows, D.C., Harrison, R.M., 2016. Source apportionment of wide range particle size spectra and black carbon collected at the airport of Venice (Italy). Atmos. Environ. 139, 56–74.
Masiol, M., Harrison, R.M., Vu, T.V., Beddows, D., 2017. Sources of sub-micrometre particles near a major international airport. Atmos. Chem. Phys. 17 (20), 12379–12403.
Mazaheri, M., Johnson, G.R., Morawska, L., 2009. Particle and gaseous emissions from commercial aircraft at each stage of the landing and takeoff cycle. Environ. Sci. Tech. 43 (2), 441–446.
McBride, G.B., 2005. A proposal for strength-of-agreement criteria for Lin's concordance correlation coefficient. NIWA client report: HAM2005-062, 45, pp.307-310.
Møller, K.L., Thygesen, L.C., Schipperijn, J., Loft, S., Bonde, J.P., Mikkelsen, S., Brauer, C., 2014. Occupational exposure to ultrafine particles among airport employees-combining personal monitoring and global positioning system. PLoS One 9 (9), e106671.
Moreno-Ríos, A.L., Tejeda-Benítez, L.P., Bustillo-Lecompte, C.F., 2022. Sources, characteristics, toxicity, and control of ultrafine particles: An overview. Geosci. Front. 13 (1), 101147.
Nieminen, T., Kerminen, V.M., Petäjä, T., Aalto, P.P., Arshinov, M., Asmi, E., Baltensperger, U., Beddows, D.C., Beukes, J.P., Collins, D., Ding, A., 2018. Global analysis of continental boundary layer new particle formation based on long-term measurements. Atmos. Chem. Phys. 18 (19), 14737–14756.
Oliveira, T.P., Moral, R.A., Zocchi, S.S., Demetrio, C.G., Hinde, J., 2020. Lcc: an R package to estimate the concordance correlation, Pearson correlation and accuracy over time. PeerJ 8, e9850.
Ozili, P.K., 2023. The acceptable R-square in empirical modelling for social science research. In Social research methodology and publishing results: a guide to non-native English speakers (pp. 134-143). IGI Global.
QGIS Development Team, 2022. QGIS Geographic Information System. Open Source Geospatial Foundation Project. [Online]. Available at: https://qgis.org [Accessed: 3 April 2023].
QtiPlot. 2008. QtiPlot: Data analysis and scientific visualization [Online]. Available at: https://www.qtiplot.com/ [Accessed: 3 April 2023].
R Core Team, 2013. R: A language and environment for statistical computing. R Foundation for Statistical Computing, Vienna, Austria.
Riley, K., Cook, R., Carr, E., Manning, B., 2021. A systematic review of the impact of commercial aircraft activity on air quality near airports. City Environment Interactions 11, 100066.
Rivas, I., Beddows, D.C., Amato, F., Green, D.C., Järvi, L., Hueglin, C., Reche, C., Timonen, H., Fuller, G.W., Niemi, J.V., Pérez, N., 2020. Source apportionment of particle number size distribution in urban background and traffic stations in four European cities. Environ. Int. 135, 105345.
Rogers, F., Arnott, P., Zielinska, B., Sagebiel, J., Kelly, K.E., Wagner, D., Lighty, J.S., Sarofim, A.F., 2005. Real-time measurements of jet aircraft engine exhaust. J. Air Waste Manage. Assoc. 55 (5), 583–593.
Rose, C., Collaud Coen, M., Andrews, E., Lin, Y., Bossert, I., Lund Myhre, C., Tuch, T., Wiedensohler, A., Fiebig, M., Aalto, P., Alastuey, A., 2021. Seasonality of the particle number concentration and size distribution: a global analysis retrieved from the network of Global Atmosphere Watch (GAW) near-surface observatories. Atmos. Chem. Phys. 21 (22), 17185–17223.
Saha, P.K., Reece, S.M., Grieshop, A.P., 2018. Seasonally varying secondary organic aerosol formation from in-situ oxidation of near-highway air. Environ. Sci. Tech. 52 (13), 7192–7202.
Saha, P.K., Zimmerman, N., Malings, C., Hauryliuk, A., Li, Z., Snell, L., Subramanian, R., Lipsky, E., Apte, J.S., Robinson, A.L., Presto, A.A., 2019. Quantifying high-resolution spatial variations and local source impacts of urban ultrafine particle concentrations. Sci. Total Environ. 655, 473–481.
Schraufnagel, D.E., 2020. The health effects of ultrafine particles. Exp. Mol. Med. 52 (3), 311–317.
Seidler, J., Friedrich, M.N., Thomas, C.K., Nölscher, A.C., 2023. Introducing the novel concept of cumulative concentration roses for studying the transport of ultrafine particles from an airport to adjacent residential areas. Egusphere 2023, 1–30.
Solomon, P.A., Vallano, D., Lunden, M., LaFranchi, B., Blanchard, C.L., Shaw, S.L., 2020. Mobile-platform measurement of air pollutant concentrations in California: performance assessment, statistical methods for evaluating spatial variations, and spatial representativeness. Atmos. Meas. Tech. 13 (6), 3277–3301.
Soppa, V., Lucht, S., Ogurtsova, K., Buschka, A., López-Vicente, M., Guxens, M., Weinhold, K., Winkler, U., Wiedensohler, A., Held, A., Lüchtrath, S., Cyrys, J., Kecorius, S., Gastmeier, P., Wiese-Posselt, M., Hoffmann, B., 2023. The berlin-brandenburg air study—a methodological study paper of a natural experiment investigating health effects related to changes in airport-related exposures. Int J Public Health 68, 1606096. https://doi.org/10.3389/ijph.2023.1606096.
Squizzato, S., Cazzaro, M., Innocente, E., Visin, F., Hopke, P.K., Rampazzo, G., 2017. Urban air quality in a mid-size city—PM2. 5 composition, sources and identification of impact areas: From local to long range contributions. Atmos. Res. 186, 51–62.
Stacey, B., Harrison, R.M., Pope, F., 2020. Evaluation of ultrafine particle concentrations and size distributions at London Heathrow Airport. Atmos. Environ. 222, 117148.
Stacey, B., Harrison, R.M., Pope, F.D., 2023. Emissions of ultrafine particles from civil aircraft: dependence upon aircraft type and passenger load. NPJ Climate Atmos. Sci. 6 (1), 161.
Stafoggia, M., Cattani, G., Forastiere, F., di Bucchianico, A.D.M., Gaeta, A., Ancona, C., 2016. Particle number concentrations near the Rome-Ciampino city airport. Atmos. Environ. 147, 264–273.
Ström, J., Engvall, A.C., Delbart, F., Krejci, R., Treffeisen, R., 2009. On small particles in the Arctic summer boundary layer: observations at two different heights near Ny-Ålesund, Svalbard. Tellus b: Chem. Phys. Meteorol. 61 (2), 473–482.
Sulo, J., Sarnela, N., Kontkanen, J., Ahonen, L., Paasonen, P., Laurila, T., Jokinen, T., Kangasluoma, J., Junninen, H., Sipilä, M., Petäjä, T., 2021. Long-term measurement of sub-3 nm particles and their precursor gases in the boreal forest. Atmos. Chem. Phys. 21 (2), 695–715.
Trebs, I., Lett, C., Krein, A., Junk, J., 2023. Air quality impacts of aviation activities at a mid-sized airport in central Europe. Atmos. Pollut. Res. 14 (3), 101696.
Trechera, P., Garcia-Marlès, M., Liu, X., Reche, C., Pérez, N., Savadkoohi, M., Beddows, D., Salma, I., Vörösmarty, M., Casans, A., Casquero-Vera, J.A., 2023. Phenomenology of ultrafine particle concentrations and size distribution across urban Europe. Environ. Int. 172, 107744.
Tremper, A.H., Jephcote, C., Gulliver, J., Hibbs, L., Green, D.C., Font, A., Priestman, M., Hansell, A.L., Fuller, G.W., 2022. Sources of particle number concentration and noise near London Gatwick Airport. Environ. Int. 161, 107092.
Ungeheuer, F., van Pinxteren, D., Vogel, A.L., 2021. Identification and source attribution of organic compounds in ultrafine particles near Frankfurt International Airport. Atmos. Chem. Phys. 21 (5), 3763–3775.
Ungeheuer, F., Caudillo, L., Ditas, F., Simon, M., van Pinxteren, D., Kılıç, D., Rose, D., Jacobi, S., Kürten, A., Curtius, J., Vogel, A.L., 2022. Nucleation of jet engine oil vapours is a large source of aviation-related ultrafine particles. Commun. Earth Environ. 3 (1), 319.
Wiesner, A., Pfeifer, S., Merkel, M., Tuch, T., Weinhold, K., Wiedensohler, A., 2020. Real world vehicle emission factors for black carbon derived from longterm in-situ measurements and inverse modelling. Atmos. 12 (1), 31.
Wing, S.E., Larson, T.V., Hudda, N., Boonyarattaphan, S., Fruin, S., Ritz, B., 2020. Preterm birth among infants exposed to in utero ultrafine particles from aircraft emissions. Environ. Health Perspect. 128 (4), 047002.
Wolf, K., Cyrys, J., Harcinícková, T., Gu, J., Kusch, T., Hampel, R., Schneider, A., Peters, A., 2017. Land use regression modeling of ultrafine particles, ozone, nitrogen oxides and markers of particulate matter pollution in Augsburg, Germany. Sci. Total Environ. 579, 1531–1540.
World Health Organization, 2021. WHO global air quality guidelines: particulate matter (PM2. 5 and PM10), ozone, nitrogen dioxide, sulfur dioxide and carbon monoxide: executive summary.
Wu, A.H., Fruin, S., Larson, T.V., Tseng, C.C., Wu, J., Yang, J., Jain, J., Shariff-Marco, S., Inamdar, P.P., Setiawan, V.W., Porcel, J., 2021. Association between airport-related

ultrafine particles and risk of malignant brain cancer: A multiethnic Cohort study. Can. Res. 81 (16), 4360–4369.
Yang, Z., Freni-Sterrantino, A., Fuller, G.W., Gulliver, J., 2020. Development and transferability of ultrafine particle land use regression models in London. Sci. Total Environ. 740, 140059.
Yun, X., Shen, G., Shen, H., Meng, W., Chen, Y., Xu, H., Ren, Y., Zhong, Q., Du, W., Ma, J., Cheng, H., 2020. Residential solid fuel emissions contribute significantly to air pollution and associated health impacts in China. Sci. Adv. 6 (44), p.eaba7621.